Received: 7 September 2021 | Revised: 15 December 2021 | Accepted: 19 December 2021

DOI: 10.1002/esp.5321

RESEARCH ARTICLE

ESPL WILEY

Disturbance and valley confinement: Controls on floodplain large wood and organic matter jam deposition in the Colorado Front Range, USA

Molly R. Guiney | Katherine B. Lininger

Department of Geography, University of Colorado Boulder, Boulder, CO, USA

Correspondence
Molly R. Guiney, Department of Geography, University of Colorado Boulder, Boulder, CO 80309, USA.
Email: molly.guiney@colorado.edu

Funding information
Colorado Scientific Society; Colorado Water Center; Geography Department (University of Colorado Boulder)

Abstract

Organic matter dynamics (entrainment, transport, deposition) can influence ecogeomorphic complexity in rivers. However, the depositional controls on downed large wood (LW) and coarse particulate organic matter (CPOM) on floodplains have rarely been assessed. We investigate the influence of different disturbance histories, as well as geomorphology and forest stand density, on the deposition of LW and CPOM accumulations, or jams, between two adjacent drainages (West Creek, North Fork Big Thompson) in the semi-arid Colorado Front Range, USA. Both basins recently experienced an extreme flood, but West Creek experienced a larger flood peak as well as a recent upstream fire. We also analyse jam fabric (LW piece orientation) between floodplain and in-channel jam types. We measured LW and CPOM jams on the North Fork to compute jam frequencies (jams ha^{-1}) and loads (volume per area; m^3 ha^{-1}), and we compare these data to a previously published dataset from West Creek. Average floodplain LW jam frequencies (70.4 jams ha^{-1}) and loads (678.6 m^3 ha^{-1}) on West Creek were significantly higher than on the North Fork (frequency: 14.8 jams ha^{-1}; load: 94.3 m^3 ha^{-1}). Average floodplain CPOM jam frequencies (West Creek: 19.0 jams ha^{-1}; North Fork: 15.1 jams ha^{-1}) and loads (West Creek: 10.70 m^3 ha^{-1}; North Fork: 9.98 m^3 ha^{-1}) were not significantly different between basins. A larger flood peak, likely enhanced by a recent upstream fire and a more confined valley bottom, resulted in greater deposition of LW jams on West Creek compared to the North Fork. Geomorphic characteristics, such as valley confinement and slope, also influence jam frequencies and loads. Floodplain jam types oriented parallel to the stream were significantly different than other jam types. This work will inform river restoration efforts using wood and organic matter and provide insight on the transport and depositional processes influencing floodplain LW jam formation.

KEYWORDS
Colorado, fire, flood, floodplain, large wood, organic matter

1 | INTRODUCTION

Downed large wood (LW; >1 m in length, >0.1 m in diameter) and coarse particulate organic matter (CPOM; >1 mm in diameter, smaller than LW) can enhance ecogeomorphic complexity on floodplains. In addition to being a large carbon stock in river corridors (Lininger et al., 2017; Sutfin et al., 2016), organic matter and LW contribute critical nutrients to floodplain soils, stimulating riparian growth (Pettit & Naiman, 2005, 2006). Organic matter on floodplains also provides animals, such as rodents, birds, and reptiles, with food sources and habitat (Fauteux et al., 2012; Harmon et al., 1986; Laven & Mac Nally, 1998; Pettit & Naiman, 2006; Sperry & Weatherhead, 2010; Swihart & Slade, 1985). Geomorphically, floodplain LW influences overbank flows, promoting sedimentation, secondary channel

formation, and ultimately the establishment of microtopography on floodplains (Jeffries et al., 2003; Sear et al., 2010). These effects are likely enhanced when LW pieces are aggregated into jams, as jams on floodplains may be more stable and persistent over time than individual LW pieces (Abbe & Montgomery, 1996). CPOM (i.e., twigs, leaves, small wood pieces, etc.) can influence floodplain geomorphic complexity by accumulating with LW jams, reducing jam porosity and thereby increasing the stability and impact of jams on channel and floodplain morphology (Schalko et al., 2018). It is also likely that CPOM influences the hydraulic roughness of floodplains when concentrated into jams. A large body of work investigates the dynamics (entrainment, transport, and deposition) of in-channel LW (Comiti et al., 2016; Ruiz-Villanueva et al., 2019), as well as the geomorphic impacts of disturbances, such as floods and fires (Brogan et al., 2019; Magilligan et al., 2015; Sholtes et al., 2018), but the influence of disturbance on LW and CPOM delivery onto floodplains has not been adequately explored. We compare the influence of different disturbance histories, as well as geomorphic and forest stand characteristics, on the fluvial deposition of LW and CPOM jams. We also characterize and compare floodplain LW jam types.

Fluvially deposited (allochthonous) floodplain jams can form by LW and CPOM racking up against impediments such as floodplain trees (Lininger et al., 2021). In addition, floodplain jams have been observed as forming through congested LW transport (Ruiz-Villanueva et al., 2019), although the gradual formation of floodplain LW jams could also potentially occur during uncongested transport. Greater flood discharges likely increase transport capacity (Comiti et al., 2016) and the potential for deposition onto floodplains, and floods that trigger floodplain erosion can recruit additional wood to the channel for transport (Benda & Sias, 2003; Comiti et al., 2016; Steeb et al., 2017). Recent fires may also enhance LW recruitment, transport, and deposition by influencing flood magnitude and the potential for hillslope failures (Comiti et al., 2016; King et al., 2013; Moody et al., 2013). Previous work suggests that recent high-magnitude disturbances can influence spatial distributions of floodplain LW (Iskin & Wohl, 2021; Lininger et al., 2021; Wohl, Cadol, et al., 2018). However, questions remain about the types and magnitudes of disturbances required to cause significant LW deposition onto floodplains. In-channel CPOM dynamics have been well-studied (Bilby & Likens, 1980; Iroumé et al., 2020; Quinn et al., 2007; Wallace et al., 1995; Wohl et al., 2019), but we lack understanding of CPOM deposition onto floodplains during disturbances.

Geomorphic and forest stand characteristics also influence floodplain LW and CPOM deposition. Limited work suggests that confinement (channel width to valley bottom width) influences floodplain LW volume per area (i.e., loads) (Galia et al., 2020; Wohl, Cadol, et al., 2018), though the direction of this relationship varies. In some locations, more confined reaches resulted in lower floodplain LW loads (Wohl, Cadol, et al., 2018), and in other locations the opposite trend was observed (Galia et al., 2020). Increasing drainage area has been associated with lower LW jam frequencies, and reaches with lower slopes can have higher LW and CPOM jam loads (Lininger et al., 2021). The hydrologic regime (perennial vs. intermittent) influences floodplain LW deposition, where intermittent streams have had smaller LW loads (Galia et al., 2020). Multithread channels are correlated with greater in-channel LW loads due to lower transport capacities (Gurnell et al., 2000; Wohl, Scott, et al., 2018; Wyżga et al., 2017). However, we know of only one study that has investigated how floodplain LW loads vary with channel planform, with no difference being found between planform types (Wohl, Scott, et al., 2018). Increased forest stand density has been associated with increased CPOM jam frequencies and loads (Lininger et al., 2021), whereas open woodland floodplains may allow for greater LW transport onto floodplains (Lininger et al., 2021; Wohl, Cadol, et al., 2018).

The fluvial deposition of LW onto floodplains may create distinct jam types, and identifying jam types can inform our understanding of the mechanics of floodplain LW transport and deposition. In-channel LW jam types have previously been identified in the Pacific Northwest, USA (Abbe & Montgomery, 1996, 2003), and some studies have noted the presence of strandline jams along floodplain margins (Piégay, 1993; Piégay & Gurnell, 1997). However, no comprehensive jam-type classification exists for floodplain LW jams, and studies assessing LW piece orientation in jams (jam fabric) are limited.

We investigate the influence of disturbance history and geomorphic characteristics on the frequencies and loads of floodplain LW and CPOM jams in two adjacent drainages in the Colorado Front Range. The North Fork Big Thompson River (North Fork) and West Creek experienced an extreme precipitation event and flood in 2013, but the flood peak was higher on West Creek compared to the North Fork (Yochum & Moore, 2013), and West Creek also experienced a fire upstream of the study area in 2010. The differences in disturbance type and magnitude between these basins offer a rare opportunity to compare the influence of disturbance histories, and a multi-basin assessment of the influence of geomorphic characteristics and forest stand density on floodplain jam frequencies and loads may provide a more comprehensive understanding of jam deposition. We also explore LW jam types identified in the field to expand our understanding of floodplain jam dynamics.

Much of the LW dynamics research has focused on in-channel LW, which may pose a threat to communities and infrastructure during floods (Ruiz-Villanueva et al., 2016). Conversely, floodplain LW jams may be more stable and CPOM jams less harmful if mobilized than in-channel LW. Thus, understanding floodplain LW and CPOM jam dynamics may likely prove beneficial in the context of stream management and restoration, since LW and CPOM on floodplains can provide ecological benefits (e.g., carbon storage, nutrients and habitat) (Fauteux et al., 2012; Pettit & Naiman, 2006; Sutfin et al., 2016) with reduced hazard. Investigating jam fabric and jam types may also offer insight into the transport and depositional processes of jams on floodplains, as well as provide concrete examples of jam deposition that may improve the outputs of numerical models incorporating LW transport and deposition.

1.1 | Objectives

We frame our analyses around three objectives. First, we seek to quantity differences in jam frequencies and loads between watersheds with varying disturbance histories. Large floods can introduce substantial inputs of LW into the river corridor (Comiti et al., 2016; Ruiz-Villanueva et al., 2019). Because West Creek experienced a larger flood peak magnitude compared to the North Fork in the 2013 flood, we expect that H1: West Creek will have greater floodplain LW and CPOM jam frequencies and loads than the North Fork.

Second, we aim to determine the geomorphic controls that influence jam deposition. There are only a few studies that have investigated the influence of reach-scale geomorphic characteristics on floodplain jams (Galia et al., 2020; Lininger et al., 2021; Wohl, Cadol, et al., 2018), and the influence of planform characteristics (e.g., sinuosity and multithread vs. single-thread channels) on floodplain jam deposition has not been adequately explored. In addition, we assess how geomorphic characteristics (e.g., valley confinement, slope) may influence jam deposition on floodplains. We hypothesize that H2a: More confined reaches (with a greater ratio of channel width to valley bottom width) will be correlated with lower floodplain jam loads and H2b: Reaches with multithread planforms will have greater floodplain jam frequencies and loads.

Third and finally, we seek to identify and compare distinct LW jam types on floodplains to in-channel jam types. We expect that H3a: Jam fabric (LW piece orientation) will differ by jam type identified in the field. Strandline jams, as defined above, generally orient parallel to the stream (Piégay, 1993; Piégay & Gurnell, 1997), and jam fabric may be influenced by transport characteristics (i.e., trapping mechanisms, location in channel, transport regime, etc.), as suggested by lab experiments (Bocchiola et al., 2006; Braudrick et al., 1997). Floodplain jams incorporating both allochthonous LW and autochthonous LW (not fluvially deposited) in the Congaree National Park (South Carolina, USA) had no distinct orientations (Wohl et al., 2011), but we suspect that our identified allochthonous jam types will orient in distinct directions. We also expect that H3b: Inclination, or the vertical angle relative to a horizontal plane, of LW pieces in jams will differ by jam type. For example, LW jams within the floodplain margin and interior may have greater piece inclinations than in-channel LW jams due to trapping mechanisms on floodplains forcing LW pieces to adjust during deposition.

2 | STUDY AREA

We conducted fieldwork during summer 2020 in the Colorado Front Range. The Front Range is characterized by a semi-arid mountain climate, and all fieldwork was conducted in the upper montane ecosystem (elevation range from ~1750 to 2850 m). Precipitation ranges from 116 to 825 mm annually (Colorado Climate Center, 2019). Temperatures range between 10 and 22.5°C in summer and −10 and 0°C in winter (Sibold et al., 2006; Veblen & Donnegan, 2005). The Front Range experiences a snowmelt season through the spring and early summer months, and monsoonal summer thunderstorms frequently occur in the area (Sibold et al., 2006). Many river networks consist of alternating reaches of confined and unconfined segments (Beechie et al., 2006; Bellmore & Baxter, 2014; Wohl, Lininger, et al., 2018). Forest stands are primarily composed of ponderosa pine (*Pinus ponderosa*) and Douglas fir (*Pseudotsuga menziesii*) (Buechling & Baker, 2004; Veblen & Donnegan, 2005).

We conducted the majority of our fieldwork in the North Fork drainage (Figure 1), measuring floodplain and in-channel jams and reach characteristics. On West Creek, we identified jam types and measured LW jam fabric and in-channel LW jam loads. We also incorporated data on floodplain LW and CPOM jam frequencies and loads on West Creek that was collected in summer 2019 and is fully described in Lininger et al. (2021). The drainages flow southeast through the Rocky Mountain National Park and Arapahoe-Roosevelt National Forest. The drainage areas at the downstream study reach for the North Fork and West Creek are 43 and 60 km^2, respectively. The Cow Creek tributary (25.3 km^2) flows into West Creek within our study region, increasing the West Creek drainage area downstream of the confluence by 80%. Elevation within the reach areas ranges from 2400 to 2800 m (North Fork) and 2270 to 2440 m (West Creek). The investigated elevation ranges vary slightly between the basins due to substantial LW removal and stream restoration occurring below 2400 m on the North Fork, but all study reaches are within the montane zone. West Creek and the North Fork have not been systematically logged since the early 1900s (Veblen & Donnegan, 2005).

The North Fork watershed is underlain by early Proterozoic biotitic schists and metasedimentary rocks, whereas West Creek is dominated by mid-Proterozoic granites. Glacial sediments and features, such as moraines and rock glaciers, exist in the headwaters of both basins upstream of our study sites (Braddock & Cole, 1990; Jones & Quam, 1944). The North Fork follows an inactive fault line, and a knickpoint exists upstream of our study regions in both rivers.

In 2010, the Cow Creek fire burned 1200 acres within the West Creek basin upstream of the knickpoint and the study locations described in Lininger et al. (2021) and used in our study. No other significant fires occurred in West Creek during the last 100 years (Buechling & Baker, 2004). After our field data were collected, a high-severity fire (Cameron Peak fire) burned portions of our North Fork study reaches. However, prior to the Cameron Peak fire, the North Fork watershed had not experienced any major fires in recent decades (Buechling & Baker, 2004).

In September 2013, an uncharacteristic weather pattern caused intense precipitation and extensive flooding across the Colorado Front Range and in the study drainages (Gochis et al., 2015; Yochum, 2015; Yochum & Moore, 2013). Our visual investigation of published precipitation maps from the 2013 event suggests that total precipitation accumulation over both basins ranged between 177.9 and 228.6 mm, and the annual probabilities of exceedance for the worst-case 24-hour precipitation were visually estimated to be between 1/200 and 1/500 for the North Fork and 1/500 and 1/1000 for West Creek (Gochis et al., 2015). However, precipitation intensities were not measured directly within the basins during the event. These two watersheds are not gauged, but Yochum and Moore (2013) estimated flood recurrence intervals by measuring cross-sections determined by high-water marks (bent grass, slackwater deposits) and using the critical depth method to calculate discharge. The estimated flood discharge was compared to the 100-year discharge calculated using regional regression equations of peak flow (Capesius & Stephens, 2009; Yochum & Moore, 2013) to approximate recurrence intervals. On West Creek, the estimate of peak discharge just upstream of Glen Haven was 311.5 $m^3\ s^{-1}$, equivalent to four times the approximated 100-year flood (Yochum & Moore, 2013). On the North Fork, the estimate of peak discharge upstream of Glen Haven was 48.1 $m^3\ s^{-1}$, approximated as a 50- to 100-year flood (Yochum & Moore, 2013).

Although our data were collected between 2019 and 2020, evidence of the flood is still apparent because the flood was so extreme, and there were no similar events between 2013 and when the data were collected. On West Creek, the flood eroded substantial portions of the floodplain, and in some places exposed bedrock in the channel.

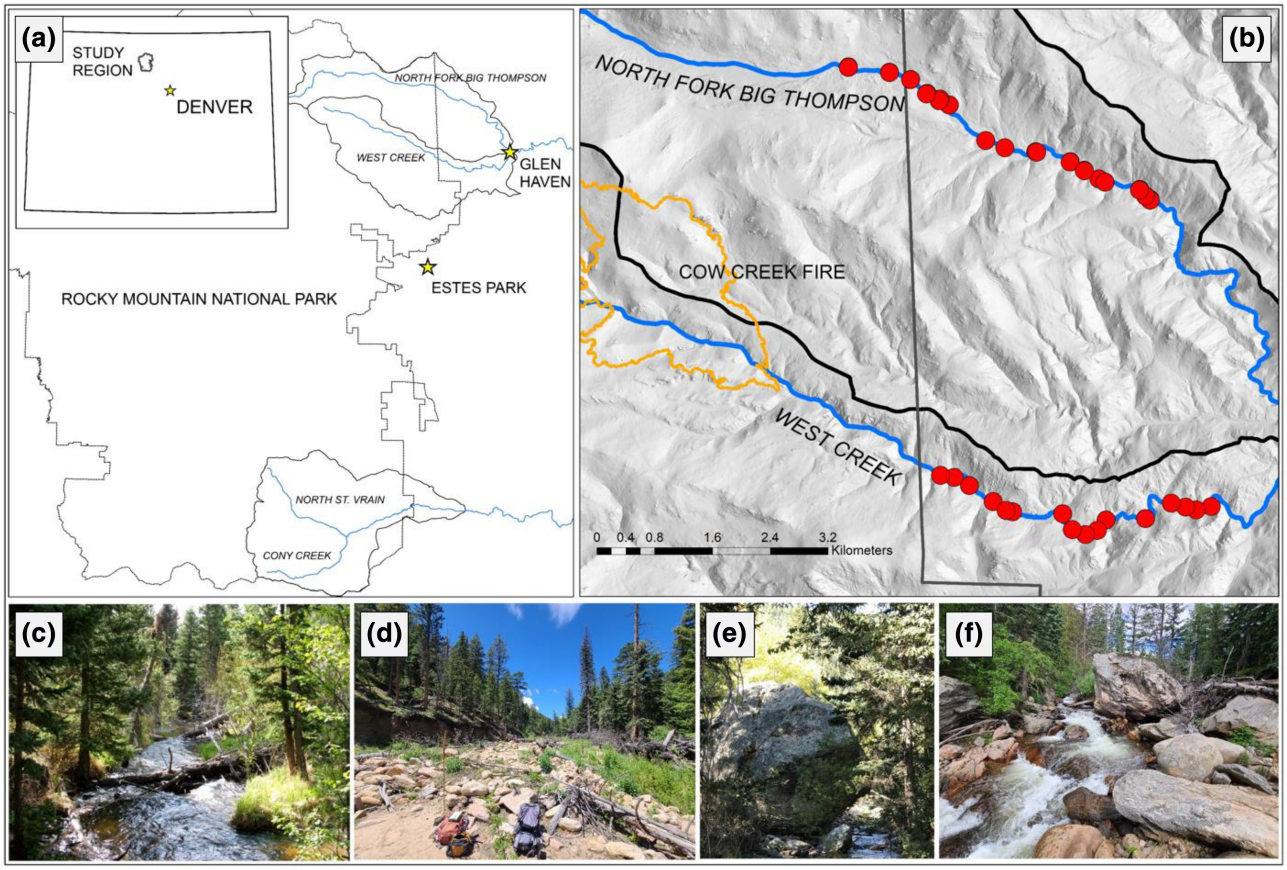

FIGURE 1 Map of study area depicting (a) watershed locations within the state of Colorado, (b) study reaches (red dots) and recent fires along West Creek (from Lininger et al., 2021) and the North Fork, (c, d) West Creek before and after the 2013 flood, and (e, f) the North Fork before and after the 2013 flood. Note that before-and-after photos were not taken in the same locations. Before photo on West Creek taken by Joe Grim (http://joeandfrede.com/); before photo on the North Fork obtained from https://www.alltrails.com/trail/us/colorado/north-fork-big-thompson-river-trail-via-dunraven-trailhead/photos [Color figure can be viewed at wileyonlinelibrary.com]

Channel avulsions occurred and cobble bars formed in old channels and meanders. Flood scars on trees are present, as well as overbank sediment deposits. The flood event also initiated a large debris flow in the burned region of West Creek upstream of our study sites (Coe et al., 2014), and we noted smaller hillslope failures during fieldwork. On the North Fork, channel widening and floodplain erosion also occurred (DeWitt, 2016). Abandoned flood channels and coarse sediment deposits are apparent on floodplain surfaces. No debris flows were noted along the North Fork during fieldwork.

Few in-channel LW jams exist in the North Fork and West Creek, so we measured in-channel LW jam types and fabric on the North St. Vrain and Cony Creek near Allenspark, CO to compare floodplain and in-channel jam types of the upper montane elevation range. A full description of these additional sites is included in Text S1 in the online Supporting Information.

3 | METHODS

3.1 | Data collection

On the North Fork, we identified 16 study reaches in which to measure floodplain jam frequencies and loads using stratified random sampling (see Text S2 in the online Supporting Information for a full description). For each reach, we measured the bankfull channel width (m; refers to the 1- to 2-year flow channel, post-2013 flood) at 25 m increments along the reach using a laser range finder (TruPulse 360B), averaging these measurements for each reach. Bankfull width measurements included the sum of all channels in multithread reaches. We also measured water surface slope (m m^{-1}) using the laser range finder. We measured total valley bottom width at each 25 m increment using a metre tape and averaged the results for a reach-averaged valley bottom width. During the valley bottom width measurements, we measured standing tree basal area (m^2 ha^{-1}), which indicates forest stand density, every 10 m along the metre tape perpendicular to the channel using a Panama Angle Gauge. Only living trees in the valley bottom were initially included, but dead trees were incorporated into later reach measurements. A short analysis of the impact of including dead standing trees partway through the field season is included in Text S3 in the online Supporting Information. Basal area measurements along the transects were averaged to create one basal area value per reach.

Drainage area (km^2) was obtained using the StreamStats website maintained by the USGS (U.S. Geological Survey, 2016). Sinuosity (channel length/valley length) was measured in Google Earth using 2019 satellite imagery. Valley bottom area (ha) was calculated by multiplying the reach-averaged valley width by reach length. If islands were present in the channel, island area was added to the valley bottom area. Some side-channel widths and island areas were not fully measured in the field. To account for this, bankfull width and island

area were estimated via aerial imagery in Google Earth in a few reaches. We calculated a confinement index for each reach as the ratio of channel width to valley bottom width.

In addition to geomorphic characteristics and forest stand density, we measured all LW and CPOM jams on the floodplain ($n = 150$) and any in-channel LW jams within the reaches ($n = 11$). We only included allochthonous, fluvially deposited jams in our analyses, which we identified by determining whether a jam showed evidence of transport (see Text S4 in the online Supporting Information for examples of identification criteria). All jams were required to be greater than 0.5 m in at least two dimensions. Jams containing three or more pieces of LW, with less than 75% CPOM and sediment (visual estimate), were identified as LW jams (Figure 2). Jams with fewer than three pieces, or jams comprised of greater than 75% CPOM and sediment, were identified as CPOM jams. Some jams were part of a multi-jam complex, connected by one or multiple LW pieces. If jams were connected by only one LW piece, jams were recorded as distinct jams. If jams were connected by two or more LW pieces, jams were considered as one singular jam. If jams were connected by two or more LW pieces but could be classified differently (i.e., a CPOM jam and a LW jam), these jams were recorded separately for the purpose of analysing differences in jam loads and characteristics between LW and CPOM jams.

We measured jam characteristics including the horizontal distance from and elevation above the edge of the bankfull channel (m); the most common decay class of LW pieces in the jam (using a scale from Scott et al., 2019 ranging from 1 = least decay to 5 = most decay; see Text S5 in the online Supporting Information for a full description of decay classes); and the number of pins, or objects trapping the jam, such as trees. Total blockage (cm), or the sum of all pin diameters at breast height, was calculated using a metre tape. We also measured the total volume of LW and CPOM in jams for each reach. The volume (m^3) of each jam was calculated by estimating jam dimensions using a best-fit box and then visually estimating porosity to determine the volume of LW or CPOM in jams (Livers et al., 2020). Length (dimension parallel to the channel), width (dimension perpendicular to the channel) and height were measured with a measuring tape or laser range finder. Then, two investigators made estimates of the porosity within the best-fit box, resulting in a calculation of LW or CPOM jam volume in the box. The two porosity estimates were averaged to reduce systematic error in porosity estimations (see Figure S1 for a comparison of the two estimates). Volumes were summed to get the total LW and CPOM volume in jams per reach. In addition to floodplain jams, we measured in-channel LW jams located within the reaches to compare proportions of floodplain to channel jam loads. Like the floodplain LW jam data collection, we measured jam characteristics including jam volume, CPOM percentage and number of pins. Channel area (ha) was calculated by multiplying the reach-averaged bankfull width by reach length.

We calculated the following reach-level jam variables with our field data: LW and CPOM jam frequency (jams ha^{-1}), LW and CPOM jam loads (m^3 ha^{-1}), and average LW and CPOM jam size (m^3) for each reach. Floodplain LW and CPOM jam counts and loads were normalized to valley bottom area (excluding the channel area), whereas in-channel LW jams were normalized to channel area. The proportion of floodplain to in-channel LW loads in jams was calculated for each reach.

To compare our data collected on the North Fork to West Creek, we used a previously published dataset of 16 reaches from West Creek (Lininger et al., 2021) that contains the same measurements and variables collected on the North Fork. Floodplain LW and CPOM

FIGURE 2 Examples of floodplain jams: (a, b) LW jams on West Creek, (c) CPOM jam on West Creek, and (d) CPOM jam on the North Fork [Color figure can be viewed at wileyonlinelibrary.com]

loads from the West Creek dataset were measured on the floodplain on one side of the river channel, so we recalculated the confinement index by measuring the total valley bottom width of each reach on West Creek using aerial imagery and digital elevation models (DEMs) in ArcGIS. One reach on the North Fork also only includes data from one side of the river channel due to the encroachment of the 2020 Cameron Peak Fire in the region and our inability to access the site. We similarly determined the reach confinement index using aerial imagery and DEMs. Because our jam variables (jam frequency and load) are normalized by floodplain area, we can compare data between West Creek and the Nork Fork. In addition, in-channel LW jam data were not reported in Lininger et al. (2021), so we measured in-channel LW jams in the West Creek reaches as described for the North Fork.

For our third research objective, we measured the orientation of LW pieces in 35 floodplain LW jams along West Creek and the North Fork, and 12 in-channel LW jams on the North St. Vrain and Cony Creek. We measured in-channel jams on the North St. Vrain and Cony Creek due to the lack of in-channel jams on West Creek and the North Fork. We identified six different jam types in the field (Figure 3): floodplain margin strandline jams, located on floodplain margins and containing many LW pieces that appear to orient parallel to the channel; floodplain margin transverse jams, located on floodplain margins and containing many LW pieces that appear to orient perpendicular to the channel; floodplain margin irregular jams, located on floodplain margins and containing no obvious jam orientation; floodplain interior irregular jams, located within floodplain interiors with no obvious jam orientation; in-channel transverse jams, in which many of the LW pieces appeared oriented perpendicular to the channel; and in-channel irregular jams, in which there was no obvious jam orientation. Some jams had multiple parts connected by more than two LW pieces with what appeared to be different orientations between parts. We separated these jams into distinct parts to better understand differences in orientation. We measured the azimuth, or compass bearing, of every accessible LW piece in the jams using a laser range finder (accuracy: ±1°). We also measured the azimuth of the stream near each jam using Google Earth and 2019 satellite imagery. Inclination, the angle a LW piece is oriented relative to a horizontal plane, was also measured for every LW piece (accuracy: ±0.25°), along with jam characteristics such as jam volume, number of pins, and the presence of rootwads.

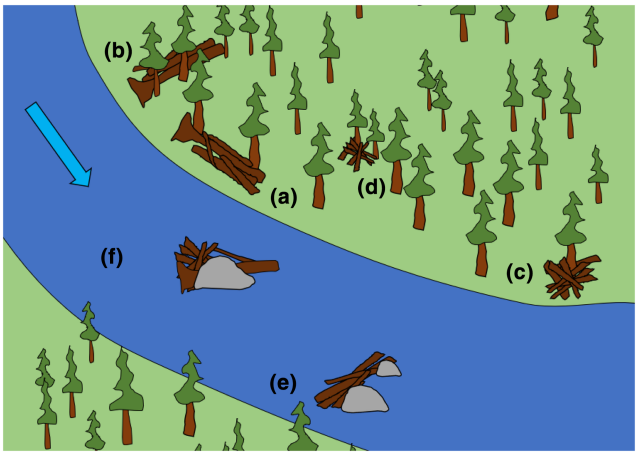

FIGURE 3 Illustration of jam types: (a) floodplain margin strandline, (b) floodplain margin transverse, (c) floodplain margin irregular, (d) floodplain interior irregular, (e) in-channel transverse and (f) in-channel irregular. Blue arrow refers to stream flow [Color figure can be viewed at wileyonlinelibrary.com]

3.2 | Analyses

We conducted analyses of jam frequencies and loads using R (R Core Team, 2020), analysing LW and CPOM jam variables separately. To investigate the influence of differing disturbance regimes between basins on floodplain jam deposition, we compared LW and CPOM jam frequencies (jams ha^{-1}) and jam loads (m^3 ha^{-1}) between basins using the Wilcoxon rank sum test. To assess the geomorphic and forest stand controls on floodplain jam deposition, we first conducted univariate analyses. We investigated associations using Spearman rank correlation tests and Wilcoxon rank sum tests between jam frequencies and jam loads and the following reach-level variables: drainage area, slope, confinement index, sinuosity, bankfull width, basal area, whether a reach was multithread or not (Y or N) and river (West Creek, North Fork). We tested for geomorphic and forest stand differences between the North Fork and West Creek to characterize the drainages. We also tested for jam-level differences between the North Fork and West Creek, including the distance from and elevation above the channel at which jams were located, the number of pins trapping a jam, and total blockage per jam. We conducted multiple linear regressions using the response variables of jam loads and jam frequencies with the reach-level predictor variables listed above. Predictor variables were tested for multicollinearity using the Spearman rank correlation test prior to regression analyses and through the variance inflation factor (VIF) test (Thompson et al., 2017). If correlations were significant and the Spearman statistic ρ was greater than 0.8, variables were removed from the model. If VIF values were greater than approximately 4, variables were also systematically removed until the VIFs of the remaining variables were below 4. Because the categorical river variable was highly correlated with various geomorphic variables, including confinement and slope, the variable was removed from our analyses. The jam frequency response variables were square-root-transformed, and the load response variables were log1p-transformed.

We completed model selection using the dredge function from the MuMIn package (Barton, 2020). The dredge function uses the full model (with all variables) to subset variables in different combinations to determine the rank of best-fit models. Ranks are decided according to the Akaike information criterion corrected for small sample sizes (AICc). Akaike weights were also calculated to determine the importance of predictor variables within the full models (Wagenmakers & Farrell, 2004). We identified all models within a two-unit range from the lowest AICc and from these, the model with the fewest predictor variables was chosen as the final model. If multiple models had the fewest number of predictor variables, the final model was then chosen as the model with the variables that had the highest Akaike weights. Final models were checked for significant outliers using the Cook's distance test. One reach was found to significantly influence both the CPOM jam frequency and jam load model results. However, we did not remove the outlier reach due to the limited number of data points (16 reaches per river). Residuals were also checked for normality and homoscedasticity. All tests and models were evaluated at a significance level of 0.05 ($\alpha = 0.05$), but significance levels of $\alpha = 0.1$ are

also reported to capture additional patterns and trends that are present in the data at slightly higher significance levels (Krueger & Heck, 2019).

To analyse jam fabric between jam types identified in the field, each LW piece orientation was normalized to the stream orientation measured for the jam in question. We then combined all LW piece orientations across all jams within each jam type. For example, all LW pieces within floodplain margin transverse jams were combined into one larger distribution for analysis. We used the Oriana circular statistics program (Kovach, 2011) to plot jam type distributions and calculate distribution statistics, such as mean orientation. We plotted data on rose diagrams and compared each jam type distribution of LW pieces to a uniform distribution using the Watson U^2 single-sample test to indicate preferential alignment. Jam type distributions were also compared to one another using the two-sample version of the Watson U^2 test, with a Bonferroni correction applied for multiple comparisons (adjusted $\alpha = 0.003$).

We also calculated the percentage of LW pieces in each jam type that were oriented relatively parallel and relatively perpendicular to the stream (Figure S2). LW pieces oriented between 0 and 45°, 135 and 225°, or 315 and 360° were considered relatively parallel, while LW pieces oriented between 45 and 135° or 225 and 315° were considered relatively perpendicular. Other calculations, such as summary statistics and comparisons of piece inclination by jam type, were completed in R.

4 | RESULTS

4.1 | Comparison of jam loads and frequencies between drainage basins

We measured a total of 150 allochthonous jams on the North Fork floodplain with nearly equal numbers of LW jams ($n = 79$) and CPOM jams ($n = 71$). We found only eight in-channel LW jams on the North Fork, and only three in-channel LW jams on West Creek across all reaches. Summary statistics for jam characteristics on the North Fork are included in Table S1 in the online Supporting Information, and correlations between reach-level and jam-level variables are included in Tables S2–S4 and in Figure S3. For an in-depth description of floodplain jam characteristics on West Creek, see Lininger et al. (2021).

The geomorphic characteristics and forest stand density differ between the two basins (Table 1). On the North Fork, slope was on average higher than on West Creek ($p = 0.007$) and had a wider range of values (Figure 4). Average slope on the North Fork was 0.07 m m^{-1} (median = 0.06 m m^{-1}), while average slope on West Creek was 0.03 m m^{-1} (median = 0.03 m m^{-1}). Sinuosity was slightly higher on West Creek ($p = 0.001$), likely due to the occasional bedrock outcrops forcing the river's path. Sinuosity averaged 1.20 (median = 1.13) on West Creek and 1.06 (median = 1.04) on the North Fork, demonstrating that both streams are relatively straight.

Basal area was also greater on average on the North Fork ($p = 0.017$), though West Creek exhibited a wide range of values. Mean basal area on the North Fork was 15.01 m^2 ha^{-1} (median = 14.43 m^2 ha^{-1}) and 10.55 m^2 ha^{-1} (median = 9.63 m^2 ha^{-1}) on West Creek. Despite the North Fork having many complex multithread channel reaches ($n = 10$) while West Creek had none, bankfull width was not significantly different between the rivers. Confinement index was significantly different at $\alpha = 0.1$ between basins ($p = 0.068$), with the North Fork generally having wider valley bottoms (mean = 0.28, median = 0.20) relative to West Creek (mean = 0.40, median = 0.32). Because the bankfull width was similar between basins, the difference in confinement between basins is likely driven by the valley bottom width.

Floodplain LW jam frequencies and loads were significantly higher on West Creek compared to the North Fork (frequency: $p < 0.001$, load: $p = 0.002$; Figure 5). However, CPOM jam frequencies and loads were not significantly different between West Creek and the North Fork. The proportion of in-channel LW jams compared to floodplain LW jams was not significantly different between rivers (Table S5), likely due to the very small number of in-channel jams on both rivers. The distance at which both LW and CPOM jams were located from the bankfull channel was significantly higher on West Creek than on the North Fork (LW: $p < 0.001$; CPOM: $p < 0.001$; Figures 6a and b). The elevation at which LW and CPOM jams were located above bankfull was also higher on West Creek (LW: $p < 0.001$; CPOM: $p < 0.001$; Figures 6c and d). The number of pins trapping CPOM jams was significantly higher on the North Fork than on West Creek ($p = 0.013$), but not higher for LW jams (Figures 7a and b). Total blockage per LW jam was significantly higher on West Creek than on the North Fork ($p = 0.043$), but CPOM jam total blockage was not significantly different between basins (Figures 7c and d). West Creek had, on average, a lower decay class compared to the North Fork. The majority of LW in jams on West Creek (76.8%) was decay class 2, whereas most LW in jams on the North Fork (70.7%) was decay class 3. See Figures S4 and S5 in the online Supporting Information for additional jam-level results.

When conducting univariate analyses of floodplain jam frequencies and loads and reach-level geomorphic variables and basal area, significant relationships existed between jam frequency and drainage area, confinement index, and multithread sections. An increase in drainage area was associated with a decrease in LW jam frequency ($p = 0.051$, $\rho = -0.35$; Figure 8). No such association was found for CPOM jam frequency. In more confined reaches, LW and CPOM jam frequencies were higher (LW: $p = 0.006$, $\rho = 0.48$; CPOM: $p = 0.004$, $\rho = 0.50$; Figures 9a and b). Multithread sections were also significantly associated with LW jam frequency at $\alpha = 0.1$ ($p = 0.064$), with single-thread channels having higher LW jams per area. CPOM jam frequency was not significantly correlated with multithread reaches.

Jam loads were significantly correlated with slope, confinement index, and multithread sections. With an increase in slope, LW jam loads decreased ($p = 0.006$, $\rho = -0.48$; Figure 10). CPOM jam loads had no significant correlation with slope. In more confined reaches (higher confinement index), jam loads were higher (LW: $p = 0.039$, $\rho = 0.37$; CPOM: $p = 0.031$, $\rho = 0.38$; Figures 9c and d). Multithread channels had significantly smaller LW jam loads at $\alpha = 0.1$ than single-thread channels ($p = 0.084$), but CPOM jam loads were not significantly different between multithread and single-thread reaches.

In our multiple linear regression analyses, all chosen models for the response variables were significant ($p < 0.05$; Table 2). The final model chosen for LW jam frequency included drainage area, confinement index, and the categorical multithread variable as predictor variables, with an adjusted R^2 of 0.36. The three variables with the greatest sums of Akaike weights were drainage area (sum = 0.95),

TABLE 1 Table of geomorphic variables and basal area by reach for the North Fork and West Creek. Data of West Creek are from Lininger et al. (2021)

Reach	Reach length (m)	Drainage area (km^2)	Sinuosity ($m\ m^{-1}$)	Bankfull width (m)	Multithread	Slope ($m\ m^{-1}$)	Confinement index	Basal area ($m^2\ ha^{-1}$)
WC28	100	58.0	1.39	9.13	N	0.03	0.28	11.82
WC30	100	57.8	1.05	10.37	N	0.03	0.38	10.33
WC32	70	57.7	1.21	8.97	N	0.05	0.32	0.00
WC34	90	57.6	1.08	7.76	N	0.02	0.33	7.10
WC42	100	57.0	1.06	7.28	N	0.05	0.54	0.26
WC49	100	56.7	1.18	6.86	N	0.02	0.16	17.49
WC50	100	31.3	1.10	29.90	N	0.02	1.55	23.56
WC52	75	30.0	1.16	4.73	N	0.05	0.22	6.89
WC54	100	29.8	1.15	4.90	N	0.03	0.11	16.07
WC57	100	29.0	1.92	8.42	N	0.04	0.23	10.33
WC65	100	28.7	1.07	5.92	N	0.04	0.41	8.90
WC66	68	28.5	1.26	6.98	N	0.04	0.46	6.89
WC69	100	31.1	1.09	8.05	N	0.04	0.33	7.24
WC73	100	31.0	1.31	7.71	N	0.03	0.30	17.18
WC76	100	30.8	1.09	7.62	N	0.02	0.28	8.93
WC78	100	30.0	1.05	10.00	N	0.04	0.46	15.86
Median		**31.1**	**1.13**	**7.74**	–	**0.03**	**0.32**	**9.63**
NF2	75	42.7	1.02	9.63	N	0.04	0.38	19.35
NF3	75	42.5	1.03	9.25	N	0.02	0.20	15.09
NF4	75	42.2	1.15	9.95	N	0.04	0.20	19.30
NF10	100	41.7	1.01	6.46	N	0.05	0.62	11.96
NF11	75	41.4	1.07	7.05	Y	0.08	1.08	10.17
NF13	98	41.2	1.13	7.94	Y	0.03	0.17	13.52
NF15	100	40.4	1.06	8.06	Y	0.03	0.10	12.71
NF21	100	39.4	1.15	13.50	Y	0.03	0.09	7.44
NF26	100	36.3	1.14	7.66	N	0.06	0.06	18.78
NF29	100	35.2	1.06	6.54	N	0.06	0.02	11.32
NF36	87	29.3	1.03	8.44	Y	0.10	0.14	20.55
NF38	100	29.0	1.01	9.82	Y	0.15	0.24	19.24
NF40	100	28.7	1.01	9.54	Y	0.11	0.07	16.30
NF43	75	28.5	1.03	8.95	Y	0.10	0.37	10.60
NF46	72	24.4	1.04	13.33	Y	0.08	0.35	13.77
NF52	94	23.9	1.03	9.06	Y	0.15	0.33	20.01
Median		**37.8**	**1.04**	**9.01**	–	**0.06**	**0.20**	**14.43**

confinement index (sum = 0.80), and multithread (sum = 0.68; Table S6). In the CPOM jam frequency final model, confinement index, basal area, and bankfull width were included and the adjusted R^2 was 0.38. The sums of Akaike weights for the top three variables were 0.99 for confinement index, 0.90 for basal area, and 0.89 for bankfull width (Table S6). The final model for LW jam load contained just slope as a predictor and the adjusted R^2 was 0.11. The sums of Akaike weights for the top three variables were 0.73 for slope, 0.37 for drainage area, and 0.35 for confinement index (Table S6). The final model for CPOM jam load included predictor variables confinement index and basal area, with an adjusted R^2 of 0.15. The top three variables with the largest sums of Akaike weights were confinement index (sum = 0.73), basal area (sum = 0.64), and bankfull width (sum = 0.46; Table S6).

4.2 | Jam fabric analysis

Almost all jam types were significantly different from a uniform distribution ($p < 0.05$; Table 3, Figure 11), demonstrating preferential alignment, but in-channel irregular jams were only significantly different from a uniform distribution at $\alpha = 0.1$. When comparing distributions between jam types, the floodplain margin strandline jam type was significantly different from all other jam types, but no other significant results were found with other jam types when adjusting for multiple comparisons. The floodplain margin strandline jam type had the greatest proportion of LW pieces oriented parallel to the stream (0.62), whereas the greatest proportions of LW pieces oriented perpendicular to the stream were found in the floodplain margin transverse (0.69) and in-channel transverse jam (0.66) types. Inclination

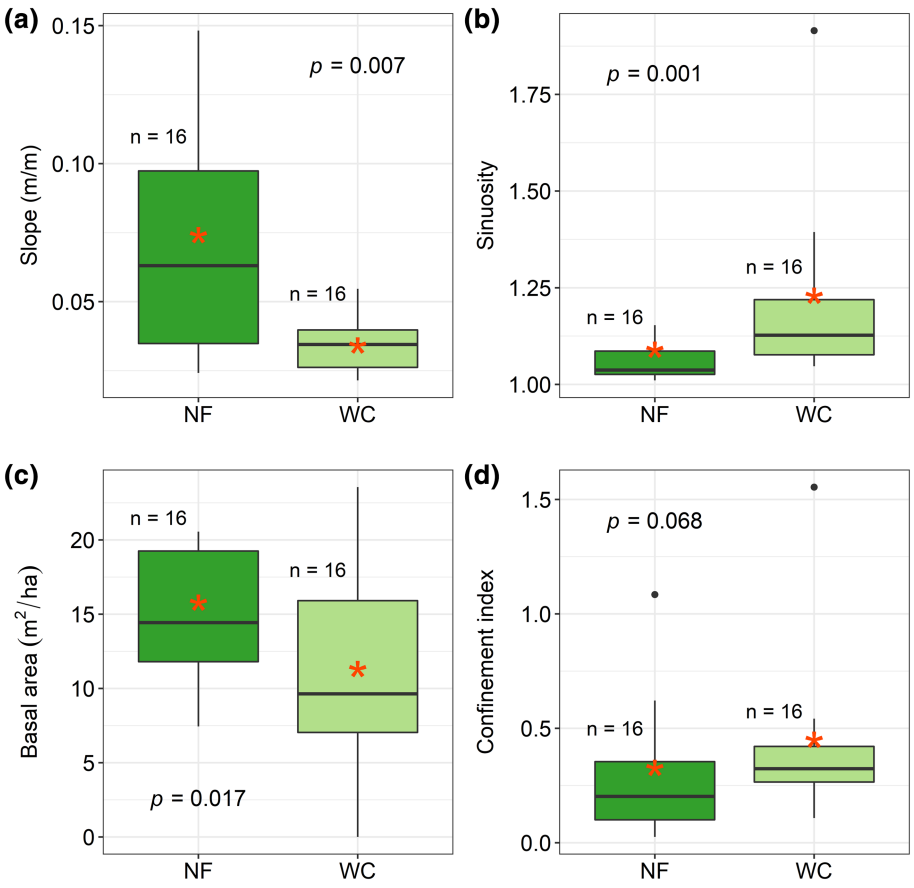

FIGURE 4 Comparison of slope (a), sinuosity (b), basal area (c), and confinement index (d) between West Creek and the North Fork. For boxplots, the orange star within the box indicates the mean value [Color figure can be viewed at wileyonlinelibrary.com]

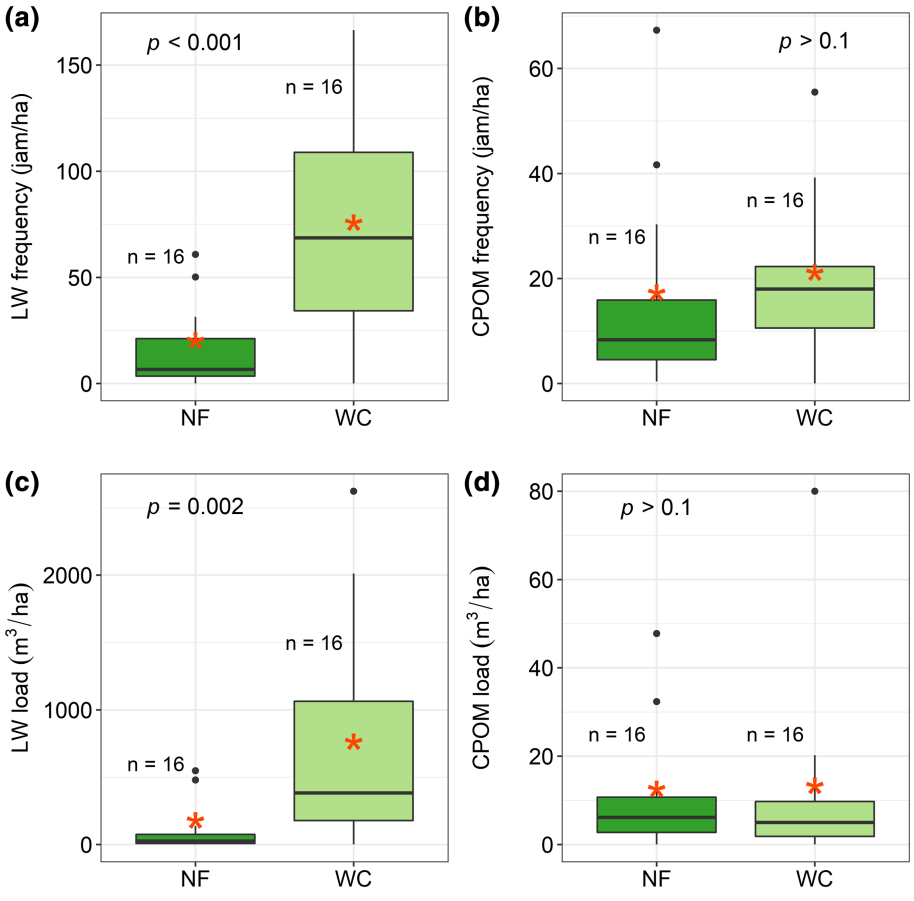

FIGURE 5 Plots of each river and (a) LW jam frequency, (b) CPOM jam frequency, (c) LW jam load and (d) CPOM jam load. For boxplots, the orange star within the box indicates the mean value [Color figure can be viewed at wileyonlinelibrary.com]

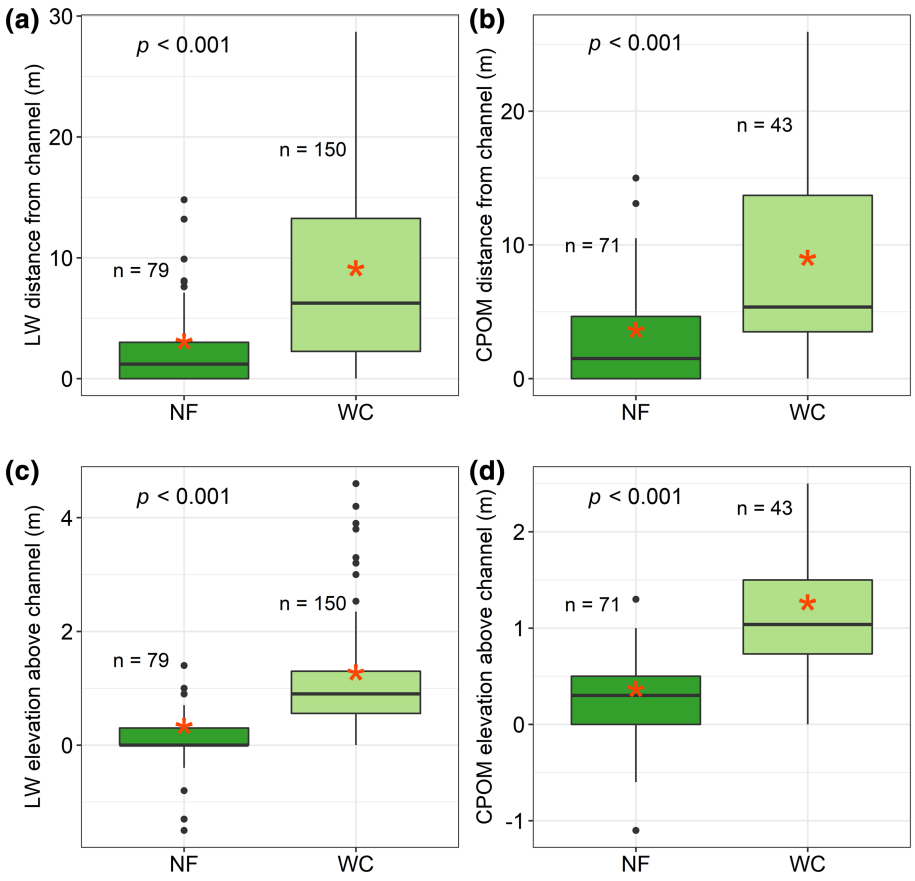

FIGURE 6 Plots of river and distance from the bankfull channel at which LW (a) and CPOM jams (b) were located; elevation above the bankfull channel at which LW (c) and CPOM (d) jams were located. For boxplots, the orange star within the box indicates the mean value [Color figure can be viewed at wileyonlinelibrary.com]

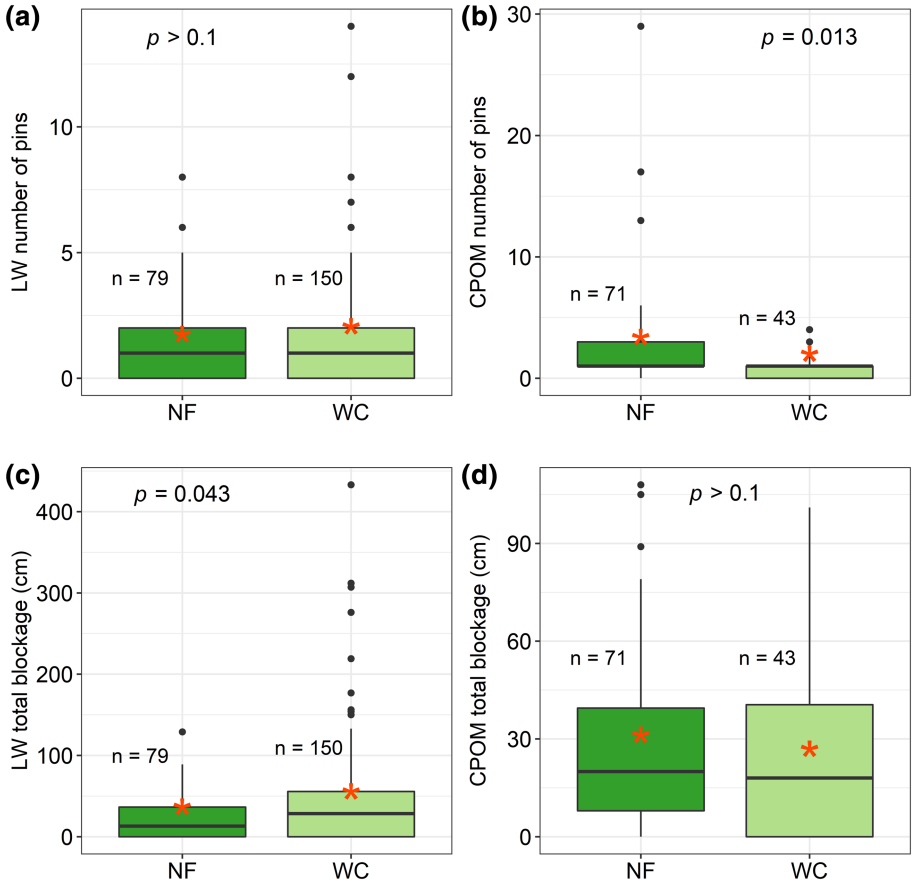

FIGURE 7 Plots of river and the number of pins trapping LW (a) and CPOM (b) jams; LW (c) and CPOM (d) total blockage. For boxplots, the orange star within the box indicates the mean value [Color figure can be viewed at wileyonlinelibrary.com]

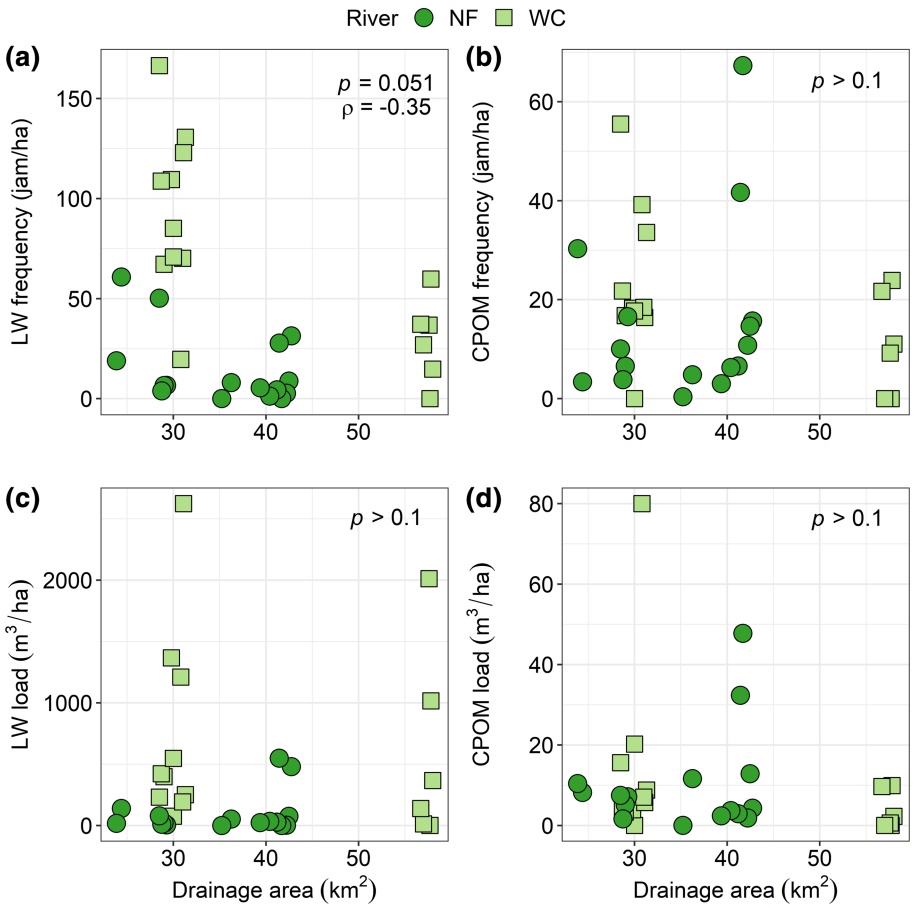

FIGURE 8 Plots of drainage area and (a) LW jam frequency, (b) CPOM jam frequency, (c) LW jam load and (d) CPOM jam load [Color figure can be viewed at wileyonlinelibrary.com]

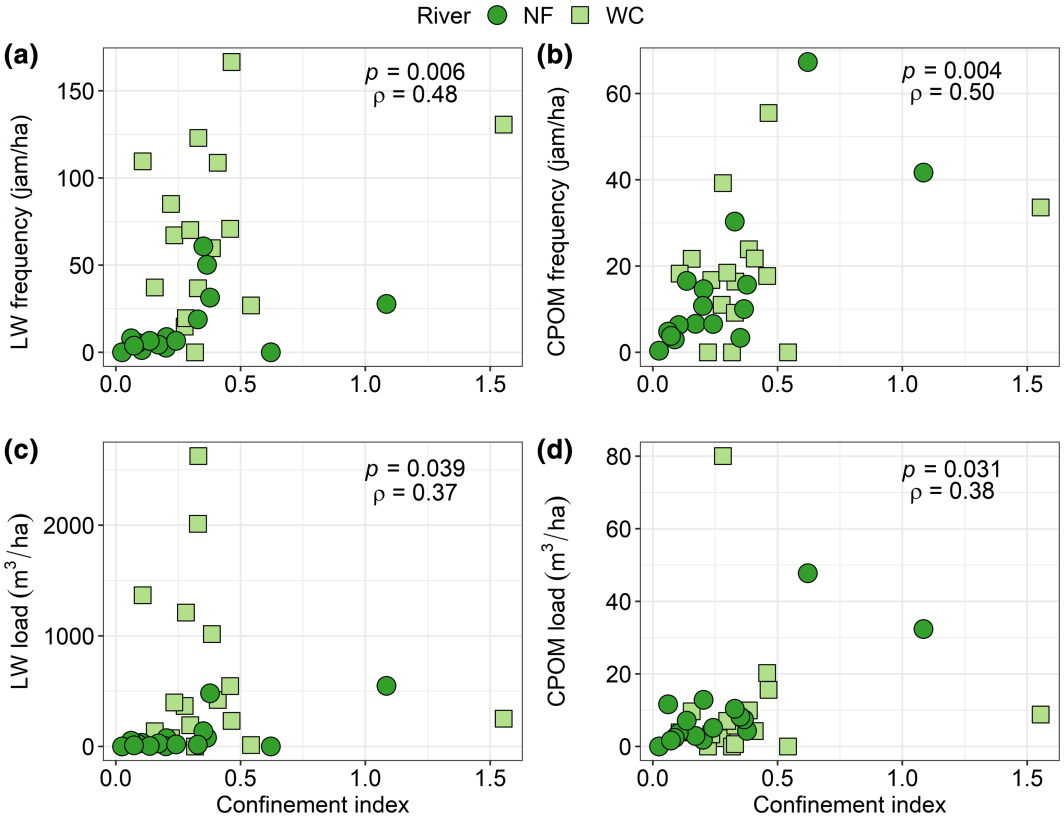

FIGURE 9 Plots of confinement index and (a) LW jam frequency, (b) CPOM jam frequency, (c) LW jam load and (d) CPOM jam load [Color figure can be viewed at wileyonlinelibrary.com]

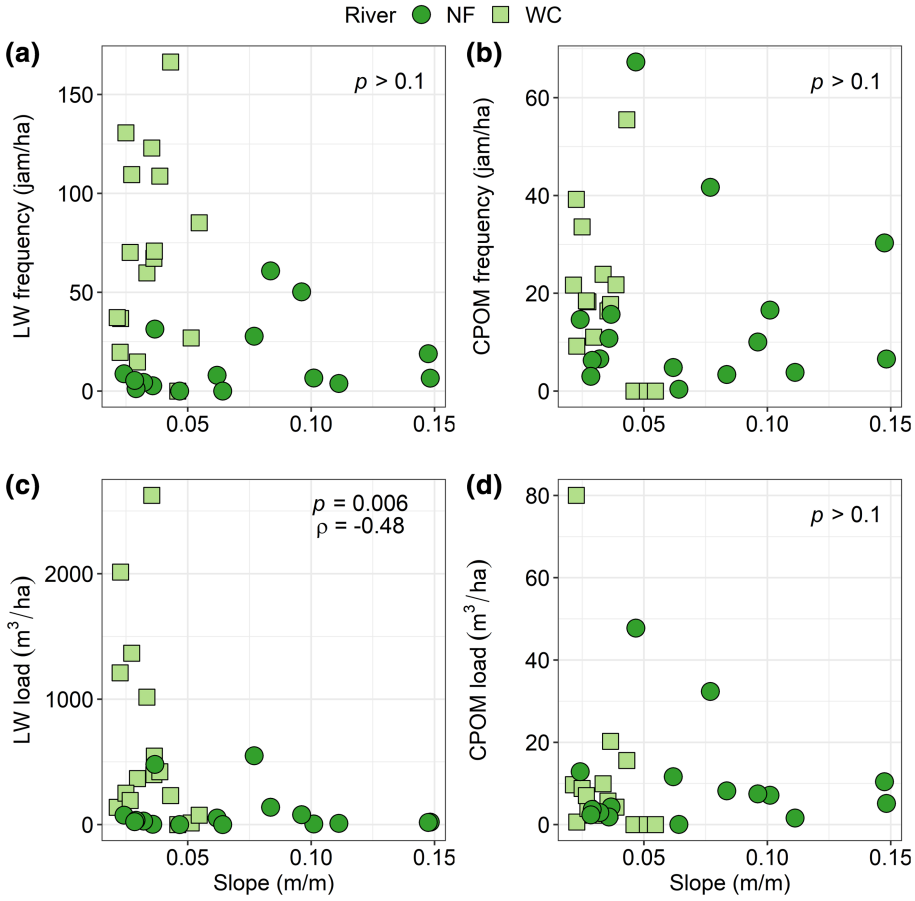

FIGURE 10 Plots of slope and (a) LW jam frequency, (b) CPOM jam frequency, (c) LW jam load and (d) CPOM jam load [Color figure can be viewed at wileyonlinelibrary.com]

TABLE 2 Final models chosen through model selection using the AICc criterion

Response variable	Variables included in final model (*p*-value) [coefficient β]	Adjusted R^2 of final model	Top variables ranked with importance
sqrt (LW frequency)	drainage area (<0.004) [−0.16] confinement index (0.027) [4.12] multithread (0.007)	0.36	drainage area, confinement index, multithread
sqrt (CPOM frequency)	confinement index (<0.001) [5.31] basal area (0.007) [0.16] bankfull width (0.009) [−0.27]	0.38	confinement index, basal area, bankfull width
log1p (LW load)	slope (0.033) [−24.48]	0.11	slope, drainage area, confinement index
log1p (CPOM load)	confinement index (0.076) [1.11] basal area (0.072) [0.06]	0.15	confinement index, basal area, bankfull width

was not significantly different between jam types ($p > 0.1$; Figure S6). Average jam size varied somewhat between jam types (Figure S7), with floodplain margin transverse jams having the greatest volume.

5 | DISCUSSION

5.1 | The influence of disturbance history on floodplain LW and CPOM jams

The results of our analysis support our hypothesis H1 that the basin with a larger peak flood magnitude (West Creek) would have greater jam frequencies and loads, but only with respect to LW jams. Larger floods have greater transport capacities, and thus greater loads of LW can be mobilized and transported onto floodplains. The distance from and elevation above the channel at which LW jams were deposited was greater on West Creek compared to the North Fork, reflecting the higher flood peak magnitude. Larger flood magnitudes may also result in greater LW jam frequencies and loads due to increased LW recruitment (Comiti et al., 2016). Recruitment of LW into the channel primarily occurs via hillslope failures and lateral bank erosion (Benda & Sias, 2003). During the 2013 flood, the extreme discharge triggered extensive floodplain and hillside erosion on West Creek, likely resulting in significant LW recruitment for transport and subsequent deposition. This probably occurred on the North Fork as well, but to a lesser degree. In addition, West Creek is more confined and connected to hillslopes compared to the North Fork. Field observations indicated that substantial hillslope failures

TABLE 3 Jam characteristics by jam type. Jam types listed in the Watson U^2 two sample test metric indicate significantly different results. Mean and median orientations are relative to the stream channel orientation

	Floodplain margin strandline	Floodplain margin transverse	Floodplain margin irregular	Floodplain interior irregular	In-channel transverse	In-channel irregular
Jam count (n)	8	8	11	8	8	4
Mean orientation (°)	154.89	106.61	81.40	112.89	89.91	84.73
Median orientation (°)	154.30	108.50	82.50	114.40	87.80	80.00
Proportion perpendicular	0.38	0.69	0.55	0.59	0.66	0.56
Proportion parallel	0.62	0.31	0.45	0.41	0.34	0.44
Mean inclination (°)	14.44	15.38	14.47	15.87	14.67	15.08
Median inclination (°)	11.60	11.50	11.00	11.90	9.80	10.80
Watson U^2 single sample	$p < 0.005$	$p < 0.005$	$p < 0.05$	$p < 0.005$	$p < 0.005$	$p < 0.1$
Watson U^2 two sample	All jam types	Floodplain margin strandline	Floodplain margin strandline	Floodplain margin strandline	Floodplain margin strandline	Floodplain margin strandline

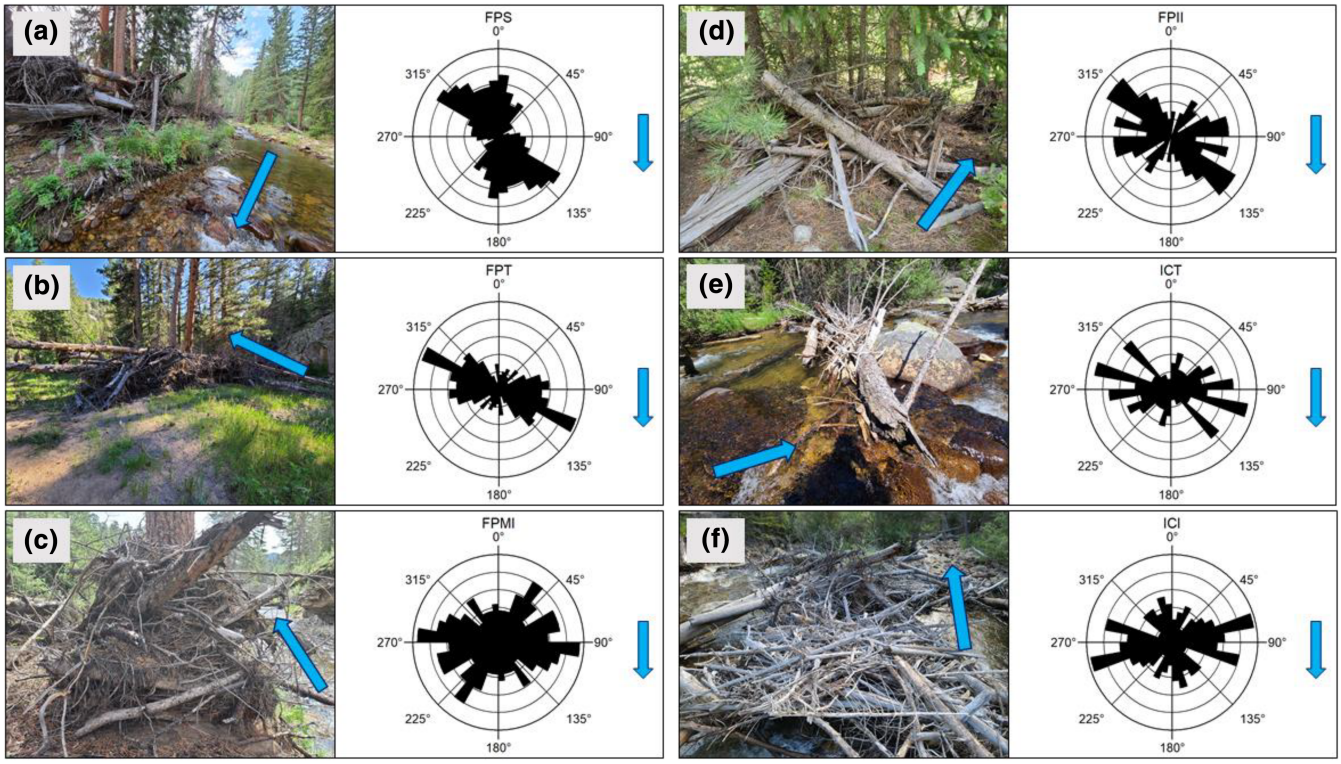

FIGURE 11 Examples of individual jams and corresponding jam fabric for each jam type: (a) floodplain margin strandline, (b) floodplain margin transverse, (c) floodplain margin irregular, (d) floodplain interior irregular, (e) in-channel transverse, and (f) in-channel irregular. Blue arrows denote streamflow direction [Color figure can be viewed at wileyonlinelibrary.com]

occurred along West Creek, also likely increasing LW recruitment. The different types and degree of recruitment spurred by the larger peak flood on West Creek may ultimately have increased the amount of LW available for transport, thus increasing deposition of LW onto floodplains. Therefore, the impact of a larger peak flood is multifaceted, in that both transport capacity and the capacity for geomorphic work (erosion and thus LW recruitment) influence LW deposition.

It is clear that peak flood magnitude likely influenced floodplain LW jam deposition, but understanding what caused the difference in peak flood magnitude between basins is more difficult. Although visual examination of annual precipitation probability exceedance maps suggests West Creek may have had a more intense precipitation event compared to the North Fork (Gochis et al., 2015), we do not have direct precipitation data from the basins and the range in total rainfall between basins is similar when assessing precipitation maps.

We suspect that a combination of the recent upstream fire and a more confined valley geometry on West Creek may have contributed to a greater peak flood magnitude, enhancing the recruitment, transport, and deposition of LW on floodplains. Fires can increase the likelihood of debris flows and generate increased runoff due to a reduction in infiltration capacity (Moody et al., 2013), and this effect is more pronounced with high-severity fires (Moody et al., 2008). Fires can also introduce substantial loads of LW to the river corridor, although the jams in the West Creek study reaches did not contain charred LW pieces (Lininger et al., 2021). Thus, the primary influence of the 2010 fire on LW dynamics downstream of the knickpoint may have been the generation of increased runoff, resulting in a greater peak flood magnitude on West Creek. The debris flow that occurred within the Cow Creek fire perimeter during the 2013 flood (Coe et al., 2014) supports the idea that the fire may have increased runoff generation. In comparison, the North Fork has had few fires in the last century prior to our 2020 field season (Buechling & Baker, 2004). A small tributary fire occurred in the upper portion of the North Fork basin in 1956, but the effect of wildfire on runoff generation is greatly reduced after just a few years (Wohl & Scott, 2017), suggesting that the effect of a small older fire would be minimal. An additional control on peak flood magnitude is valley bottom confinement (Magilligan, 1992; Surian et al., 2016). More expansive valley bottoms and floodplains can dissipate flood energy with increased hydraulic roughness and resistance, attenuating peak flows (Lininger & Latrubesse, 2016; Sholtes & Doyle, 2011; Woltemade & Potter, 1994). Thus, the narrower valley bottoms found on West Creek likely did little to dissipate the flood peak, whereas the unconfined reaches on the North Fork probably reduced flood magnitude.

Our results are supported by Wohl, Cadol, et al. (2018), who found greater proportions of floodplain LW concentrated into jams in rivers with recent high-magnitude disturbances compared to rivers with no recent disturbances in the southwestern USA. The authors also found that the proportion of in-channel LW compared to floodplain LW was lower in reaches with high-magnitude disturbances. Similarly, very few in-channel LW jams existed in the North Fork or West Creek. Previous work in the upper part of the North Fork prior to the 2013 flood suggests that many channel-spanning LW jams were present (Wohl & Beckman, 2014), but in-channel jams were less abundant in 2020. It is likely that much of the in-channel LW in the North Fork, as well as West Creek, was rearranged into floodplain LW jams or transported downstream during the 2013 flood.

Other studies examining floodplain LW loads across biomes do exist, though they incorporate autochthonous LW and dispersed LW pieces not in jams. When comparing our floodplain LW loads to these data, it is clear that the North Fork floodplain LW jam loads (mean = 94 m^3 ha^{-1}) are much more similar to other semi-arid rivers (62–250 m^3 ha^{-1}) than to the loads found on West Creek (mean = 679 m^3 ha^{-1}) and in the Pacific Northwest (380–743 m^3 ha^{-1}) (Lininger et al., 2017; Wohl, Cadol, et al., 2018; Wohl, Scott, et al., 2018). These comparisons indicate that disturbance magnitude and frequency are important influences on floodplain LW loads. Because of a shifting climate, precipitation regimes are predicted to transition from snowmelt systems to rainfall systems (Fritze et al., 2011; Stewart et al., 2005), and extended droughts may increase fuel for fires and lengthen fire seasons (Hurteau et al., 2014), increasing the likelihood of more frequent disturbances. Understanding organic matter dynamics in the context of disturbance will therefore become increasingly critical.

As noted above, West Creek had higher LW jam loads and frequencies, but there was no difference in CPOM jam loads and frequencies between basins, indicating that the difference in flood peak magnitude did not play a significant role in CPOM jam deposition. Greater flood magnitude has been associated with greater CPOM export in river channels (Wallace et al., 1995). However, because CPOM dimensions are relatively small, extreme floods above a certain magnitude may mobilize, transport, and deposit CPOM in jams effectively regardless of the differences in flood magnitudes.

In Figure 12, we present a conceptual model depicting our interpretation of the complex interactions between disturbance history, valley confinement and LW deposition in forested floodplains. Low-magnitude disturbances, such as snowmelt floods, may result in lower floodplain LW jam loads due to reduced LW recruitment and transport onto the floodplain, whereas historic precipitation and flooding,

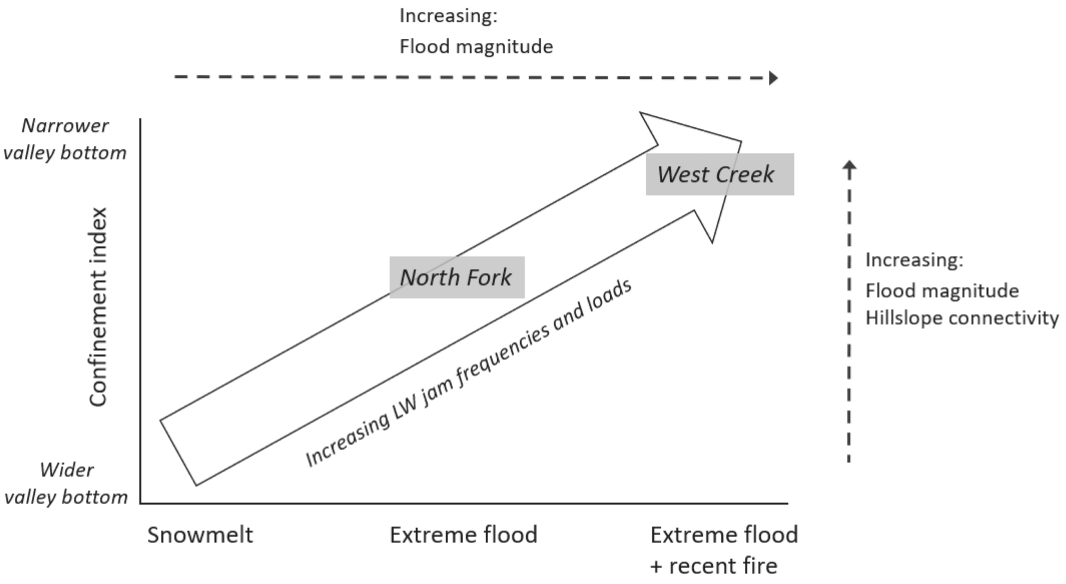

FIGURE 12 Conceptual model of the complex relationships between disturbances, geomorphology and floodplain LW jam deposition

such as the 2013 event, substantially increase LW deposition because more LW is recruited via hillslope and floodplain erosion. Historic floods, coupled with recent fires, have the potential to recruit more LW and may result in the greatest floodplain LW loads. However, flood magnitude and LW deposition are also influenced by the confinement of the valley bottom. As valley bottoms narrow, flood peak levels increase due to the reduced capacity for flood peak attenuation, increasing LW recruitment and transport. Hillslope–channel connectivity may also increase in confined valley bottoms, magnifying LW recruitment from hillslopes.

5.2 | The influence of geomorphic and forest stand characteristics on floodplain LW and CPOM jams

In addition to disturbance regime, geomorphic characteristics and forest stand density influence patterns of jam deposition. As discussed above, confinement differences between basins may influence flood peak magnitudes. In addition, confinement variations within a basin also influence where LW and CPOM jams are deposited in the river corridor. Wider valley bottoms were associated with reduced LW and CPOM jam frequencies and loads (Table 1, Figure 9), which does not support our hypothesis H2a that wider valley bottoms relative to channel width would result in increased floodplain jam frequencies and loads. In more unconfined reaches, it is less likely that a flood would extend across the entire valley bottom, and standing vegetation likely impedes LW transport further into the floodplain, resulting in smaller jam frequencies and loads when normalized by area. Our results differ from those of Wohl, Cadol, et al. (2018), who found that wider valley bottoms were associated with larger floodplain and in-channel LW loads in semi-arid rivers, but their data also included dispersed LW pieces not contained within LW jams. Our results are supported by Galia et al. (2020), who found that wider valley bottoms resulted in lower LW loads in the Mediterranean, though these results also included dispersed and autochthonous LW. The relationship we found between confinement index and floodplain LW jams could change when incorporating autochthonous LW on the floodplain, because autochthonous LW is not dependent on a flood's ability to transport material across the floodplain, but on forest processes of mortality and tree fall (Wohl, 2020).

Forest stand density also influences floodplain jam deposition. There were no significant correlations between our response variables and basal area, which indicates forest stand density. However, basal area was included as a predictor in the final model for both CPOM jam frequencies and loads, which may be related to the greater sourcing of CPOM in sites with greater basal area (Galia et al., 2020) and the importance of trees acting as trapping locations (Lininger et al., 2021). We also hypothesized that multithread reaches would have significantly larger jam frequencies and loads (H2b), but our results suggest single-thread channels have slightly greater LW jam frequencies and loads. Multithread planforms can have higher in-channel LW loads due to a lower transport capacity (Wohl, 2011; Wyżga et al., 2017), and thus we expected greater deposition of floodplain LW jams in multithread reaches. However, our data suggest that multithread channels may be less influential for floodplain LW and CPOM jam deposition than for in-channel LW jam deposition, and more work is needed to understand how planform affects floodplain jam processes.

Sinuosity was not associated with LW and CPOM floodplain deposition according to our analyses. However, previous work has shown that sinuosity, coupled with lower bank heights, may promote LW deposition on floodplains (Piégay & Marston, 1998), and the outer edge of bends can experience significant erosion and recruit additional LW to the channel during floods (Lassettre et al., 2008). It is likely that the range of sinuosity on West Creek and the North Fork was not large enough to determine any associations with floodplain LW and CPOM deposition.

Drainage area and slope were significantly associated with LW on floodplains (Figure 13). As described in Lininger et al. (2021), reaches with lower slopes may have experienced lower stream power during the flood, promoting deposition. Our results support this, where decreasing slope results in greater LW loads. However, increasing drainage area, which corresponds to decreasing slope in the drainage basins, is associated with lower LW jam frequencies. Further investigation indicates a significant correlation between slope and average LW jam size ($p = 0.001$, $\rho = -0.54$). These data ultimately indicate that with increasing drainage area and decreasing slope, LW jams are less frequent but larger in size.

The higher decay class of LW pieces on the North Fork also indicates different processes behind jam formation. On West Creek, LW pieces may have been recruited and deposited in relatively rapid events such as hillslope failures or floodplain erosion during the flood, resulting in fresher LW pieces. Conversely, in-channel and autochthonous floodplain downed LW may have been a larger source of LW in jams on the North Fork, where the flood may have remobilized and rearranged more decayed LW pieces.

The number of pins trapping CPOM jams was significantly greater on the North Fork, likely due to a higher forest stand density on the North Fork. However, total blockage was significantly greater on West Creek, suggesting that although West Creek had a lower forest stand density and jams were pinned by fewer trees, trees within the forest stands along West Creek may be larger than those on the North Fork and more effective at trapping LW in transport.

5.3 | Differences among jam types

Our expectation that jam types identified in the field would differ by jam fabric (H3a) was partially supported by our results. Although jam fabric distributions were only significantly different between

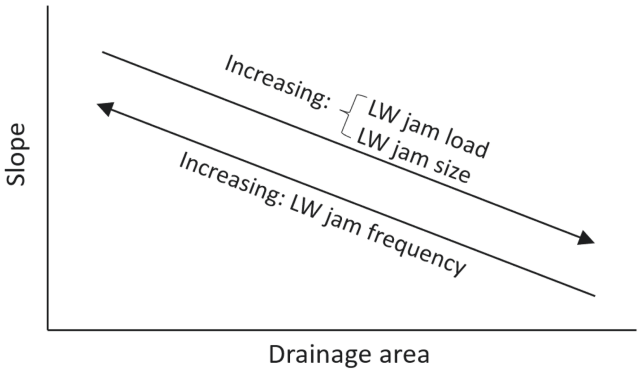

FIGURE 13 Figure of the relationships between slope, drainage area and LW jam deposition

floodplain margin strandline and all other jam types, all jam types were significantly different from a uniform distribution at $\alpha = 0.1$. In addition, some jam types (floodplain margin strandline and transverse, in-channel transverse) had greater alignment of pieces compared to others (irregular jam types). Our results contrast with the only other study to have analysed floodplain LW fabric, which found no preferential alignment in floodplain jams in the southeastern USA (Wohl et al., 2011). This may be due to the authors' potential inclusion (and our exclusion) of autochthonous LW, which may have more random orientations.

Floodplain and in-channel jam types in this study likely represent different transport regimes and depositional processes, with in-channel LW jams representing jams formed by annual snowmelt flows rather than the extreme 2013 flood event. These jam types were more likely controlled by an uncongested transport regime, in which pieces moved without significant piece-to-piece interactions (Braudrick et al., 1997). Although it is possible that floodplain jams may also form via an uncongested transport regime and the gradual accumulation of LW pieces, semi-congested, congested, or hypercongested transport likely occurred on West Creek during the 2013 flood, resulting in fluvially deposited floodplain jams. In a congested transport regime, LW pieces move as a mass and are oriented mostly perpendicular to flow, but parallel near channel margins (Braudrick et al., 1997), which could result in distinct orientations during floodplain deposition. Highly congested, wood-laden flows (i.e., hypercongested) have been observed in steep confined mountain streams and within the southwestern USA in intermittent streams (Ruiz-Villanueva et al., 2019), and generally either require large amounts of wood in the channel or episodic inputs. It is possible that West Creek experienced pulses of congested or hypercongested transport when substantial LW delivery occurred via hillslope failures. Our jam types along the floodplain margin coincide with descriptions of log levees and jams deposited after wood-laden flows (Ruiz-Villanueva et al., 2019). When congested flows fill the channel, LW pieces along the margin can rack up again floodplain vegetation in relatively parallel orientations to stream flow, like floodplain margin strandline jams. Other, less preferentially aligned jams, such as floodplain margin irregular jams, may also form (Ruiz-Villanueva et al., 2019).

We also expected to find greater inclinations of LW pieces in floodplain jam types compared to in-channel jam types (H3b). However, our hypothesis was not supported, as LW piece inclinations throughout the floodplain and channel were remarkably similar and oriented at low inclinations. Comparing inclinations of pieces from in-channel jams formed by large floods or in different geographic regions would provide more insight.

6 | CONCLUSIONS

Understanding LW and CPOM dynamics in river corridors is important for advancing ecogeomorphic research, but floodplain LW and CPOM jam depositional characteristics have been understudied. We addressed this gap by investigating the influence of different disturbance histories, as well as geomorphology and forest stand density, on the deposition of LW and CPOM jams onto floodplains in the Colorado Front Range. We found that West Creek, which experienced a higher flood peak magnitude that was possibly enhanced by a recent upstream fire and a highly confined valley bottom, influenced the recruitment and transport of LW and resulted in the deposition of extremely high loads of fluvially deposited floodplain LW jams. Conversely, the North Fork experienced a lower peak flood magnitude, had not burned recently and has a wider valley bottom, potentially resulting in less recruitment, transport, and deposition of floodplain LW jams. CPOM jam deposition was not controlled by flood magnitude above a certain threshold, but reach-scale characteristics, such as confinement index and basal area, did play an influential role. We also compared floodplain and in-channel jam types by jam fabric (piece orientation) and other characteristics. We found that some jam types varied by jam fabric and that jam types oriented perpendicular were most preferentially aligned. Our quantification of jam fabric within mountain rivers adds to our understanding of the depositional processes, as well as transport processes, that influence floodplain LW jams, and will additionally provide concrete targets for modelling efforts that incorporate LW transport. More work is needed to investigate the dynamics (entrainment, transport, and deposition) of organic matter, particularly as a shifting climate influences the frequency and magnitude of disturbances. This work will also inform river restoration efforts, which use LW in the channel but have not yet extensively incorporated floodplain LW.

ACKNOWLEDGEMENTS

We would like to thank the Colorado Water Center, Colorado Scientific Society, and Geography Department (University of Colorado Boulder) for partially funding this work. We thank Taylor Johanemann for fieldwork assistance, and Sandra Ryan and Holly Barnard for comments on early versions of the manuscript.

CONFLICT OF INTEREST

The authors have no conflict of interest to declare.

DATA AVAILABILITY STATEMENT

Data supporting the results of this work are available in the digital repository of the University of Colorado Boulder (CU Scholar; https://scholar.colorado.edu/concern/datasets/5m60qt17s).

ORCID

Molly R. Guiney https://orcid.org/0000-0001-6055-5727
Katherine B. Lininger https://orcid.org/0000-0003-0378-9505

REFERENCES

Abbe, T.B. & Montgomery, D.R. (1996) Large woody debris jams, channel hydraulics and habitat formation in large rivers. *Regulated Rivers: Research & Management*, 12(2–3), 201–221. Available from: https://doi.org/10.1002/(SICI)1099-1646(199603)12:2/3<201::AID-RRR390>3.0.CO;2-A

Abbe, T.B. & Montgomery, D.R. (2003) Patterns and processes of wood debris accumulation in the Queets river basin, Washington. *Geomorphology*, 51(1), 81–107. Available from: https://doi.org/10.1016/S0169-555X(02)00326-4

Barton, K. (2020) MuMIn: Multi-Model Inference (Version R package version 1.43.15). Available from: https://CRAN.R-project.org/package=MuMIn. Accessed 1 September 2020.

Beechie, T.J., Liermann, M., Pollock, M.M., Baker, S. & Davies, J. (2006) Channel pattern and river-floodplain dynamics in forested mountain

river systems. *Geomorphology*, 78(1), 124–141. Available from: https://doi.org/10.1016/j.geomorph.2006.01.030

Bellmore, J.R. & Baxter, C.V. (2014) Effects of geomorphic process domains on river ecosystems: A comparison of floodplain and confined valley segments. *River Research and Applications*, 30(5), 617–630. Available from: https://doi.org/10.1002/rra.2672

Benda, L.E. & Sias, J.C. (2003) A quantitative framework for evaluating the mass balance of in-stream organic debris. *Forest Ecology and Management*, 172(1), 1–16. Available from: https://doi.org/10.1016/S0378-1127(01)00576-X

Bilby, R.E. & Likens, G.E. (1980) Importance of organic debris dams in the structure and function of stream ecosystems. *Ecology*, 61(5), 1107–1113. Available from: https://doi.org/10.2307/1936830

Bocchiola, D., Rulli, M.C. & Rosso, R. (2006) Transport of large woody debris in the presence of obstacles. *Geomorphology*, 76(1), 166–178. Available from: https://doi.org/10.1016/j.geomorph.2005.08.016

Braddock, W.A. & Cole, J.C. (1990) *Geologic map of Rocky Mountain National Park and vicinity, Colorado*. U.S. Geological Survey: Reston, VA.

Braudrick, C.A., Grant, G.E., Ishikawa, Y. & Ikeda, H. (1997) Dynamics of wood transport in streams: A flume experiment. *Earth Surface Processes and Landforms*, 22(7), 669–683. Available from: https://doi.org/10.1002/(SICI)1096-9837(199707)22:7<669::AID-ESP740>3.0.CO;2-L

Brogan, D.J., MacDonald, L.H., Nelson, P.A. & Morgan, J.A. (2019) Geomorphic complexity and sensitivity in channels to fire and floods in mountain catchments. *Geomorphology*, 337, 53–68. Available from: https://doi.org/10.1016/j.geomorph.2019.03.031

Buechling, A. & Baker, W.L. (2004) A fire history from tree rings in a high-elevation forest of Rocky Mountain National Park. *Canadian Journal of Forest Research*, 34(6), 1259–1273. Available from: https://doi.org/10.1139/x04-012

Capesius, J.P., & Stephens, V.C. (2009) *Regional Regression Equations for Estimation of Natural Streamflow Statistics in Colorado*. Scientific Investigations Report. U.S. Geological Survey: Reston, VA.

Coe, J.A., Kean, J.W., Godt, J.W., Baum, R.L., Jones, E.S., Gochis, D.J. & Anderson, G.S. (2014) New insights into debris-flow hazards from an extraordinary event in the Colorado Front Range. *GSA Today*, 24(10), 4–10. Available from: https://doi.org/10.1130/GSATG214A.1

Colorado Climate Center (2019) https://climate.colostate.edu/data_access.html. Accessed 1 February 2020.

Comiti, F., Lucía, A. & Rickenmann, D. (2016) Large wood recruitment and transport during large floods: A review. *Geomorphology*, 269, 23–39. Available from: https://doi.org/10.1016/j.geomorph.2016.06.016

DeWitt, C. (2016) *Geomorphic impacts of the 2013 Colorado Front Range flood on Black Canyon Creek and North Fork Big Thompson River*. MSc thesis, University of Washington, Seattle, WA.

Fauteux, D., Imbeau, L., Drapeau, P. & Mazerolle, M.J. (2012) Small mammal responses to coarse woody debris distribution at different spatial scales in managed and unmanaged boreal forests. *Forest Ecology and Management*, 266, 194–205. Available from: https://doi.org/10.1016/j.foreco.2011.11.020

Fritze, H., Stewart, I.T. & Pebesma, E. (2011) Shifts in Western North American snowmelt runoff regimes for the recent warm decades. *Journal of Hydrometeorology*, 12(5), 989–1006. Available from: https://doi.org/10.1175/2011JHM1360.1

Galia, T., Macurová, T., Vardakas, L., Škarpich, V., Matušková, T. & Kalogianni, E. (2020) Drivers of variability in large wood loads along the fluvial continuum of a Mediterranean intermittent river. *Earth Surface Processes and Landforms*, 45(9), 2048–2062. Available from: https://doi.org/10.1002/esp.4865

Gochis, D., Schumacher, R., Friedrich, K., Doesken, N., Kelsch, M., Sun, J., Ikeda, K., Lindsey, D., Wood, A., Dolan, B., Matrosov, S., Newman, A., Mahoney, K., Rutledge, S., Johnson, R., Kucera, P., Kennedy, P., Sempere-Torres, D., Steiner, M., Roberts, R., Wilson, J., Yu, W., Chandrasekar, V., Rasmussen, R., Anderson, A. & Brown, B. (2015) The Great Colorado Flood of September 2013. *Bulletin of the American Meteorological Society*, 96(9), 1461–1487. Available from: https://doi.org/10.1175/BAMS-D-13-00241.1

Gurnell, A.M., Petts, G.E., Harris, N., Ward, J.V., Tockner, K., Edwards, P. J. & Kollmann, J. (2000) Large wood retention in river channels: The case of the Fiume Tagliamento, Italy. *Earth Surface Processes and Landforms*, 25(3), 255–275. Available from: https://doi.org/10.1002/(SICI)1096-9837(200003)25:3<255::AID-ESP56>3.0.CO;2-H

Harmon, M.E., Franklin, J.F., Swanson, F.J., Sollins, P., Gregory, S.V., Lattin, J.D., Anderson, N.H., Cline, S.P., Aumen, N.G., Sedell, J.R., Lienkaemper, G.W., Cromack, K. & Cummins, K.W. (1986) Ecology of coarse woody debris in temperate ecosystems. In: MacFadyen, A. & Ford, E.D. (Eds.) *Advances in Ecological Research*. New York: Academic Press, pp. 133–302.

Hurteau, M.D., Bradford, J.B., Fulé, P.Z., Taylor, A.H. & Martin, K.L. (2014) Climate change, fire management, and ecological services in the southwestern US. *Forest Ecology and Management*, 327, 280–289. Available from: https://doi.org/10.1016/j.foreco.2013.08.007

Iroumé, A., Ruiz-Villanueva, V. & Salas-Coliboro, S. (2020) Fluvial transport of coarse particulate organic matter in a coastal mountain stream of a rainy-temperate evergreen broadleaf forest in southern Chile. *Earth Surface Processes and Landforms*, 45(13), 3216–3230. Available from: https://doi.org/10.1002/esp.4961

Iskin, E.P. & Wohl, E. (2021) Wildfire and the patterns of floodplain large wood on the Merced River, Yosemite National Park, California, USA. *Geomorphology*, 389, 107805. Available from: https://doi.org/10.1016/j.geomorph.2021.107805

Jeffries, R., Darby, S.E. & Sear, D.A. (2003) The influence of vegetation and organic debris on flood-plain sediment dynamics: Case study of a low-order stream in the New Forest, England. *Geomorphology*, 51(1), 61–80. Available from: https://doi.org/10.1016/S0169-555X(02)00325-2

Jones, W.D. & Quam, L.O. (1944) Glacial land forms in Rocky Mountain National Park, Colorado. *The Journal of Geology*, 52(4), 217–234. Available from: https://doi.org/10.1086/625213

King, L., Hassan, M.A., Wei, X., Burge, L. & Chen, X. (2013) Wood dynamics in upland streams under different disturbance regimes. *Earth Surface Processes and Landforms*, 38(11), 1197–1209. Available from: https://doi.org/10.1002/esp.3356

Kovach, W.L. (2011) *Oriana – Circular Statistics for Windows, ver. 4*. Pentraeth: Kovach Computing Services.

Krueger, J.I. & Heck, P.R. (2019) Putting the *p*-value in its place. *The American Statistician*, 73(supp 1), 122–128. Available from: https://doi.org/10.1080/00031305.2018.1470033

Lassettre, N.S., Piégay, H., Dufour, S. & Rollet, A.-J. (2008) Decadal changes in distribution and frequency of wood in a free meandering river, the Ain River, France. *Earth Surface Processes and Landforms*, 33(7), 1098–1112. Available from: https://doi.org/10.1002/esp.1605

Laven, N.H. & Mac Nally, R. (1998) Association of birds with fallen timber in box–ironbark forest of central Victoria. *Corella*, 22, 56–60.

Lininger, K.B. & Latrubesse, E.M. (2016) Flooding hydrology and peak discharge attenuation along the middle Araguaia River in central Brazil. *Catena*, 143, 90–101. Available from: https://doi.org/10.1016/j.catena.2016.03.043

Lininger, K.B., Scamardo, J.E. & Guiney, M.R. (2021) Floodplain large wood and organic matter jam formation after a large flood: Investigating the influence of floodplain forest stand characteristics and river corridor morphology. *Journal of Geophysical Research – Earth Surface*, 126(6), e2020JF006011. Available from: https://doi.org/10.1029/2020JF006011

Lininger, K.B., Wohl, E., Sutfin, N.A. & Rose, J.R. (2017) Floodplain downed wood volumes: A comparison across three biomes. *Earth Surface Processes and Landforms*, 42(8), 1248–1261. Available from: https://doi.org/10.1002/esp.4072

Livers, B., Lininger, K.B., Kramer, N. & Sendrowski, A. (2020) Porosity problems: Comparing and reviewing methods for estimating porosity and volume of wood jams in the field. *Earth Surface Processes and Landforms*, 45(13), 3336–3353. Available from: https://doi.org/10.1002/esp.4969

Magilligan, F.J. (1992) Thresholds and the spatial variability of flood power during extreme floods. *Geomorphology*, 5(3), 373–390. Available from: https://doi.org/10.1016/0169-555X(92)90014-F

Magilligan, F.J., Buraas, E.M. & Renshaw, C.E. (2015) The efficacy of stream power and flow duration on geomorphic responses to catastrophic flooding. *Geomorphology*, 228, 175–188. Available from: https://doi.org/10.1016/j.geomorph.2014.08.016

Moody, J.A., Martin, D.A. & Cannon, S.H. (2008) Post-wildfire erosion response in two geologic terrains in the western USA. *Geomorphology*, 95(3), 103–118. Available from: https://doi.org/10.1016/j.geomorph.2007.05.011

Moody, J.A., Shakesby, R.A., Robichaud, P.R., Cannon, S.H. & Martin, D.A. (2013) Current research issues related to post-wildfire runoff and erosion processes. *Earth-Science Reviews*, 122, 10–37. Available from: https://doi.org/10.1016/j.earscirev.2013.03.004

Pettit, N.E. & Naiman, R.J. (2005) Flood-deposited wood debris and its contribution to heterogeneity and regeneration in a semi-arid riparian landscape. *Oecologia*, 145(3), 434–444. Available from: https://doi.org/10.1007/s00442-005-0143-z

Pettit, N.E. & Naiman, R.J. (2006) Flood-deposited wood creates regeneration niches for riparian vegetation on a semi-arid South African river. *Journal of Vegetation Science*, 17(5), 615–624. Available from: https://doi.org/10.1111/j.1654-1103.2006.tb02485.x

Piégay, H. (1993) Nature, mass and preferential sites of coarse woody debris deposits in the lower Ain valley (Mollon reach), France. *Regulated Rivers: Research & Management*, 8(4), 359–372. Available from: https://doi.org/10.1002/rrr.3450080406

Piégay, H. & Gurnell, A.M. (1997) Large woody debris and river geomorphological pattern: Examples from S.E. France and S. England. *Geomorphology*, 19(1), 99–116. Available from: https://doi.org/10.1016/S0169-555X(96)00045-1

Piégay, H. & Marston, R.A. (1998) Distribution of large woody debris along the outer bend of meanders in the Ain River, France. *Physical Geography*, 19(4), 318–340. Available from: https://doi.org/10.1080/02723646.1998.10642654

Quinn, J.M., Phillips, N.R. & Parkyn, S.M. (2007) Factors influencing retention of coarse particulate organic matter in streams. *Earth Surface Processes and Landforms*, 32(8), 1186–1203. Available from: https://doi.org/10.1002/esp.1547

R Core Team. (2020) *R: A Language and Environment for Statistical Computing*. Vienna: R Foundation for Statistical Computing.

Ruiz-Villanueva, V., Mazzorana, B., Bladé, E., Bürkli, L., Iribarren-Anacona, P., Mao, L., Nakamura, F., Ravazzolo, D., Rickenmann, D., Sanz-Ramos, M., Stoffel, M. & Wohl, E. (2019) Characterization of wood-laden flows in rivers: Wood-laden flows. *Earth Surface Processes and Landforms*, 44(9), 1694–1709. Available from: https://doi.org/10.1002/esp.4603

Ruiz-Villanueva, V., Wyżga, B., Zawiejska, J., Hajdukiewicz, M. & Stoffel, M. (2016) Factors controlling large-wood transport in a mountain river. *Geomorphology*, 272, 21–31. Available from: https://doi.org/10.1016/j.geomorph.2015.04.004

Schalko, I., Schmocker, L., Weitbrecht, V. & Boes, R.M. (2018) Backwater rise due to large wood accumulations. *Journal of Hydraulic Engineering*, 144(9), 04018056. Available from: https://doi.org/10.1061/(ASCE)HY.1943-7900.0001501

Scott, D.N., Wohl, E. & Yochum, S.E. (2019) Wood Jam Dynamics Database and Assessment Model (WooDDAM): A framework to measure and understand wood jam characteristics and dynamics. *River Research and Applications*, 35(9), 1466–1477. Available from: https://doi.org/10.1002/rra.3481

Sear, D.A., Millington, C.E., Kitts, D.R. & Jeffries, R. (2010) Logjam controls on channel:floodplain interactions in wooded catchments and their role in the formation of multi-channel patterns. *Geomorphology*, 116(3), 305–319. Available from: https://doi.org/10.1016/j.geomorph.2009.11.022

Sholtes, J.S. & Doyle, M.W. (2011) Effect of channel restoration on flood wave attenuation. *Journal of Hydraulic Engineering*, 137(2), 196–208. Available from: https://doi.org/10.1061/(ASCE)HY.1943-7900.0000294

Sholtes, J.S., Yochum, S.E., Scott, J.A. & Bledsoe, B.P. (2018) Longitudinal variability of geomorphic response to floods. *Earth Surface Processes and Landforms*, 43(15), 3099–3113. Available from: https://doi.org/10.1002/esp.4472

Sibold, J.S., Veblen, T.T. & González, M.E. (2006) Spatial and temporal variation in historic fire regimes in subalpine forests across the Colorado Front Range in Rocky Mountain National Park, Colorado, USA. *Journal of Biogeography*, 33(4), 631–647. Available from: https://doi.org/10.1111/j.1365-2699.2005.01404.x

Sperry, J.H. & Weatherhead, P.J. (2010) Ratsnakes and brush piles: Intended and unintended consequences of improving habitat for wildlife? *The American Midland Naturalist*, 163(2), 311–317. Available from: https://doi.org/10.1674/0003-0031-163.2.311

Steeb, N., Rickenmann, D., Badoux, A., Rickli, C. & Waldner, P. (2017) Large wood recruitment processes and transported volumes in Swiss mountain streams during the extreme flood of August 2005. *Geomorphology*, 279, 112–127. Available from: https://doi.org/10.1016/j.geomorph.2016.10.011

Stewart, I.T., Cayan, D.R. & Dettinger, M.D. (2005) Changes toward earlier streamflow timing across western North America. *Journal of Climate*, 18(8), 1136–1155. Available from: https://doi.org/10.1175/JCLI3321.1

Surian, N., Righini, M., Lucía, A., Nardi, L., Amponsah, W., Benvenuti, M., Borga, M., Cavalli, M., Comiti, F., Marchi, L., Rinaldi, M. & Viero, A. (2016) Channel response to extreme floods: Insights on controlling factors from six mountain rivers in northern Apennines, Italy. *Geomorphology*, 272, 78–91. Available from: https://doi.org/10.1016/j.geomorph.2016.02.002

Sutfin, N.A., Wohl, E. & Dwire, K.A. (2016) Banking carbon: A review of organic carbon storage and physical factors influencing retention in floodplains and riparian ecosystems. *Earth Surface Processes and Landforms*, 41(1), 38–60. Available from: https://doi.org/10.1002/esp.3857

Swihart, R.K. & Slade, N.A. (1985) Seasonal use of brush piles by the Hispid cotton rat (*Sigmodon hispidus*). *Journal of Mammalogy*, 66(3), 577–580. Available from: https://doi.org/10.2307/1380941

Thompson, C.G., Kim, R.S., Aloe, A.M. & Becker, B.J. (2017) Extracting the variance inflation factor and other multicollinearity diagnostics from typical regression results. *Basic and Applied Social Psychology*, 39(2), 81–90. Available from: https://doi.org/10.1080/01973533.2016.1277529

U.S. Geological Survey. (2016) *The StreamStats program*. Available at http://streamstats.usgs.gov [accessed 15 March 2020].

Veblen, T.T. & Donnegan, J. (2005) *Historical Range of Variability of Forest Vegetation of the National Forests of the Colorado Front Range*. USDA Forest Service, Rocky Mountain Region and the Colorado Forest Restoration Institute: Fort Collins, CO.

Wagenmakers, E.-J. & Farrell, S. (2004) AIC model selection using Akaike weights. *Psychonomic Bulletin & Review*, 11(1), 192–196. Available from: https://doi.org/10.3758/BF03206482

Wallace, J.B., Whiles, M.R., Eggert, S., Cuffney, T.F., Lugthart, G.J. & Chung, K. (1995) Long-term dynamics of coarse particulate organic matter in three Appalachian mountain streams. *Journal of the North American Benthological Society*, 14(2), 217–232. Available from: https://doi.org/10.2307/1467775

Wohl, E. (2011) Threshold-induced complex behavior of wood in mountain streams. *Geology*, 39(6), 587–590. Available from: https://doi.org/10.1130/G32105.1

Wohl, E. (2020) Wood process domains and wood loads on floodplains. *Earth Surface Processes and Landforms*, 45(1), 144–156. Available from: https://doi.org/10.1002/esp.4771

Wohl, E. & Beckman, N. (2014) Controls on the longitudinal distribution of channel-spanning logjams in the Colorado Front Range, USA. *River Research and Applications*, 30(1), 112–131. Available from: https://doi.org/10.1002/rra.2624

Wohl, E., Cadol, D., Pfeiffer, A., Jackson, K. & Laurel, D. (2018) Distribution of large wood within river corridors in relation to flow regime in the semiarid western US. *Water Resources Research*, 54(3), 1890–1904. Available from: https://doi.org/10.1002/2017WR022009

Wohl, E., Hinshaw, S.K., Scamardo, J.E. & Gutiérrez-Fonseca, P.E. (2019) Transient organic jams in Puerto Rican mountain streams after hurricanes. *River Research and Applications*, 35(3), 280–289. Available from: https://doi.org/10.1002/rra.3405

Wohl, E., Kuzma, J.N. & Brown, N.E. (2004) Reach-scale channel geometry of a mountain river. *Earth Surface Processes and Landforms*, 29(8), 969–981. Available from: https://doi.org/10.1002/esp.1078

Wohl, E., Lininger, K.B. & Scott, D.N. (2018) River beads as a conceptual framework for building carbon storage and resilience to extreme climate events into river management. *Biogeochemistry*, 141(3), 365–383. Available from: https://doi.org/10.1007/s10533-017-0397-7

Wohl, E., Polvi, L.E. & Cadol, D. (2011) Wood distribution along streams draining old-growth floodplain forests in Congaree National Park, South Carolina, USA. *Geomorphology*, 126(1), 108–120. Available from: https://doi.org/10.1016/j.geomorph.2010.10.035

Wohl, E. & Scott, D.N. (2017) Transience of channel head locations following disturbance. *Earth Surface Processes and Landforms*, 42(7), 1132–1139. Available from: https://doi.org/10.1002/esp.4124

Wohl, E., Scott, D.N. & Lininger, K.B. (2018) Spatial distribution of channel and floodplain large wood in forested river corridors of the Northern Rockies. *Water Resources Research*, 54(10), 7879–7892. Available from: https://doi.org/10.1029/2018WR022750

Woltemade, C.J. & Potter, K.W. (1994) A watershed modeling analysis of fluvial geomorphologic influences on flood peak attenuation. *Water Resources Research*, 30(6), 1933–1942. Available from: https://doi.org/10.1029/94WR00323

Wyżga, B., Mikuś, P., Zawiejska, J., Ruiz-Villanueva, V., Kaczka, R.J. & Czech, W. (2017) Log transport and deposition in incised, channelized, and multithread reaches of a wide mountain river: Tracking experiment during a 20-year flood. *Geomorphology*, 279, 98–111. Available from: https://doi.org/10.1016/j.geomorph.2016.09.019

Yochum, S.E. (2015) Colorado Front Range flood of 2013: Peak flows and flood frequencies. In Proceedings of the 3rd Joint Federal Interagency Conference on Sedimentation and Hydrologic Modeling, Reno, NV.

Yochum, S.E. & Moore, D.S. (2013) *Colorado Front Range Flood of 2013: Peak Flow Estimates at Selected Mountain Stream Locations*. Washington, DC: U.S. Department of Agriculture.

SUPPORTING INFORMATION

Additional supporting information may be found in the online version of the article at the publisher's website.

How to cite this article: Guiney, M.R. & Lininger, K.B. (2022) Disturbance and valley confinement: Controls on floodplain large wood and organic matter jam deposition in the Colorado Front Range, USA. *Earth Surface Processes and Landforms*, 47(6), 1371–1389. Available from: https://doi.org/10.1002/esp.5321